CO2 escapes in the Laacher See region, East Eifel, Germany: application of natural analogue onshore and offshore geochemical monitoring

Frédérick Gal, Michel Brach, Gilles Braibant, Frédéric Jouin, Karine Michel

CO_2 escapes in the Laacher See region, East Eifel, Germany: application of natural analogue onshore and offshore geochemical monitoring

GAL Frédérick, BRACH Michel, BRAIBANT Gilles, JOUIN Frédéric, MICHEL Karine

BRGM (Bureau de Recherches Géologiques et Minières)

Metrology, Monitoring and Analyses Division

3 Avenue C. Guillemin

BP36009

45060 Orléans cedex 1, France

Phone : + 33 (0)2 38 64 38 86

Fax: + 33 (0)2 38 64 37 11

E-mail : f.gal@brgm.fr

Abstract

Natural analogues studies have received growing interest during preceding years in a CCS perspective. There is a strong willing to deploy robust and reliable technologies to ensure the safety and integrity of CO_2 underground storages. Here we present a dataset acquired in the Eifel volcanic district, using geochemical monitoring methods focusing on both dissolved and gaseous species. Onshore and offshore monitoring (Lake Laacher See) were performed to depict spatial behaviour of CO_2 natural releases. Additional gaseous species, mainly helium and radon, were also monitored to better assess the shapes of gas vents, using methodologies that were learned from hydrological and tectonic applications. Lake water monitoring allowed the characterisation of the water body itself, in terms of lateral heterogeneities, to evaluate the impact of CO_2 deep degassing near the bottom of the lake. The use of a dedicated sensor for monitoring in situ CO_2 partial pressure did not provide more valuable information that was learned from more classical physico-chemical parameters. From those investigations, the usefulness of geochemical monitoring is still demonstrated, but the use of complementary approaches and methods is still needed to get a powerful set of techniques able to warn in case of leakages occurring from depth.

Keywords

Natural analogue monitoring

Soil gas

Dissolved gas

CO_2

1. Introduction

During last years, studies focussing on CO_2 sequestration have known growing interest as part of climate mitigation researches (Holloway *et al.*, 2007; Wildenborg *et al.*, 2009; Winthaegen *et al.*, 2005). By them, studies dedicated to a better knowledge of natural analogues are of primary interest, as they focus either on sites where CO_2 is naturally stored at depth from many years (*e.g.* Gal *et al.*, 2010; Holloway *et al.*, 2007) or sites where underground gases migrate upwards (*e.g.* Battani *et al.*,

2010; Beaubien *et al.*, 2008). Researches performed on those analogues can bring useful information that have to be kept in mind when performing CO_2 sequestration in depleted oil/gas reservoirs or deep saline aquifers (Gale, 2004; Gapillou *et al.*, 2009; Riding and Rochelle, 2005; Winthaegen *et al.*, 2005).

Facing this perspective, several European nations have pooled their research efforts together through the Network of Excellence on Geological Storage of CO_2 "CO_2GeoNet", under a 6th Framework Programme funded by the European Commission in 2004 (Czernichowski-Lauriol *et al.*, 2009). Present work is part of the so-called Joint Research Activity Program "Monitoring Near Surface Leakage and its Impacts" (JRAP-18). Under this work package several methods were used, with special emphasize on soil/atmosphere gas monitoring with conventional and newly rapid surveying methods, microbiological impact studies and water column monitoring (Beaubien *et al.*, 2008; Jones *et al.*, 2009; Krüger *et al.*, 2009). Here we present results acquired in 2007 and 2008 in the vicinity and within the water body of the Laacher See, a maar lake emplaced in Western Germany near Koblenz. The western shore of the lake was investigated using simple and robust methodologies in order to depict soil gas contents, whereas numerous in-situ / real-time loggings were performed in the lake itself. The goal of this work was to better understand migration pathways of gases – especially CO_2 – in a complex system (onshore unsaturated and saturated zone / offshore water mass), in order to assess the potential impact of CO_2 leaking from a deep seated storage into shallow regolith.

2. Site description

The Laacher See is a volcanic structure emplaced in the still uplifting Palaeozoic Rhenish Massif at 12,900 ± 560 yr. Before Present (Giggenbach *et al.*, 1991; van der Bogaard, 1995) and forms part of the East Eifel volcanic district. Intra-plate alkali-basaltic lavas were produced within the upper mantle (Eifel plume), where partial melting enriched the lavas in gaseous species such as CO_2. During their rise up to the surface gases were partly released either in the lower crust or along faults and fractures in the upper crust. As the Palaeozoic basement was affected by NE-SW Variscan tectonics, the Pleistocene volcanic activity lead to the merge of numerous mineral waters in this area (van der Bogaard, 1995). Noble gases and carbon isotope ratios highlight a dominant mantle origin for the gases associated with mineral waters (Griesshaber *et al.*, 1992).

As a result of volcanic activity, some maars are nowadays emplaced within the Eifel district. By them, the Laacher See represents a crater filled with water to form a 2.5 x 1.8 km – 3.31 km² area, 52 m maximum depth lake that covers 27% of its drainage area (Aeschbach-Hertig *et al.*, 1996; Giggenbach *et al.*, 1991). Lake water level has varied during historic times as a result of human reworks in the 12th century (lowering of 10 m of the water level) and in the 19th century (extra 5 m lowering).

Lake Laacher See has been studied for many years either by academics or local water authorities as it is part of an environmental protected area. The water body itself is presently classified as mesotrophic to eutrophic one, and experiences at least once a year a complete seasonal overturn (holomitic character). Contrary to other lakes set in similar geological context, such as Lake Pavin in France, Lake Laacher See probably did never have a meromictic character due to its hollow coefficient. Water is of hard type and several discharges of gases – mainly CO_2 of mantle origin (Aeschbach-Hertig *et al.*, 1996; Griesshaber *et al.*, 1992) – along the eastern shore are known, either within the water column (up to 99% CO_2 in the gaseous phase; Griesshaber *et al.*, 1992) or in soils (up to 10% vol.; Langer, 1988). An annual release of about 5000 tons of CO_2 has been calculated by Aeschbach-Hertig *et al.* (1996). Sedimentation within the lake is a function of the water chemical state, varying from carbonate facies from 0 to 20-30 m depth, then clastic facies and last organic-rich clay facies in deeper parts (Bahrig, 1985).

As a result of human activities, some fields and pastures are emplaced along the western and southern shores of the lake. Especially along the western part some gas vents (mofettes) are emplaced, which were studied during the 2007 survey, whereas lake water characterization was performed during the 2008 survey (figure 1). During the 2007 survey soil gas studies were focussed in a meadow were rapid surveying methods using laser mounted on quad bike have highlighted the occurrence of CO_2 gas vents of limited extension (Jones *et al.*, 2009). A second soil gas site, Obermendig, was also surveyed, located 5 km SW from the centre of the lake. In this site a carbogaseous spring merges (Erlenbrunnen spring), which is thought to have similar gaseous content than other springs emplaced in the Laacher See region, i.e. a dominant CO_2 phase, $\delta^{13}C$ ratios between -3 and -5‰ VDPB (Vienna Pee Dee Belemnite), low pH values, high conductivities and low redox potentials. The 2008 survey was dedicated to water logging using multi-parameter CTD (Conductivity – Temperature – Depth) probe, together with water and dissolved gases recovered from the lake.

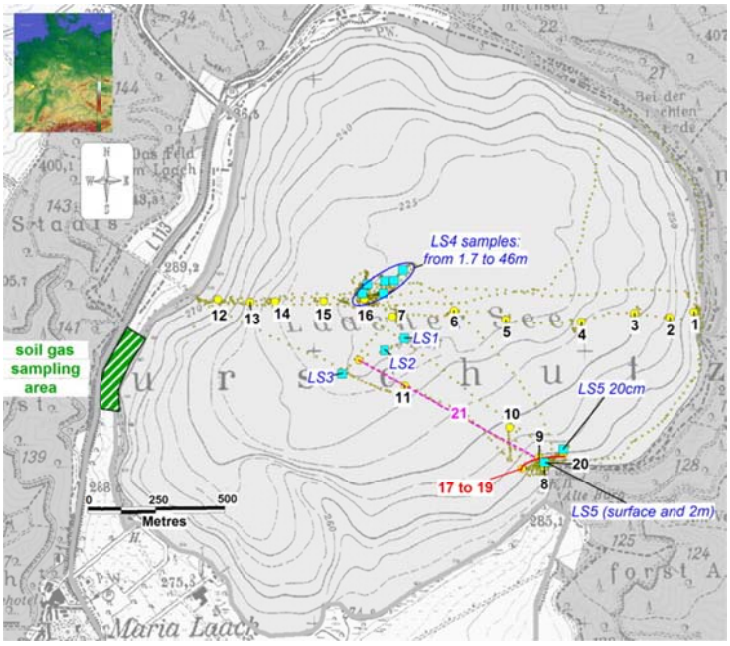

Figure 1

Site location: green dashed area: soil gas survey done in 2007; labelled yellow points: emplacement of CTD probe logging; labelled blue squares: in situ water sampling location

3. Methodology

3.1 Soil gas analyses

As reported elsewhere (*e.g.* Battani *et al.*, 2010; Gal *et al.*, 2010), there is a wide set of surveying methods that could be deployed when studying natural analogues. Here we tried to deploy robust methods in order to get reliable results that would help to interpret data acquired with more recent devices. For the 2007 soil gas survey, quantifications of CO_2, O_2, CH_4, and ^4He contents were made, as well as measurements of ^{222}Rn activities. At given locations samples for further laboratory analysis ($\delta^{13}C_{CO2}$ isotope ratio determinations and gas chromatography measurements) were also taken in evacuated glass bulbs.

Determination of soil gas species were done in the field with portable InfraRed Gas Analysers (IRGA). LFG20 (ADC Gas Analysis Ltd.) and GA2000 (Geotechnical Instruments Ltd.) gas analysers allow to determine CO_2, CH_4 and O_2 concentrations. For LFG20, detection limit is 0.05% and precisions for CO_2 and CH_4 between 0 and 10% are ± 0.5%. For GA2000, the precisions are the same between 0 and 5%, rising up to ± 1% for CO_2 and CH_4 between 5 and 15%. Calibrations of IRGA were done at

laboratory and verified on site by using CO_2 labelled bottles (from 0.05 to 100% CO_2). Sampling was done after drilling a small hole within the soil (c.a. 1 m depth, 1 cm in diameter) using a battery powered drill and inserting a copper tube in the hole. Particular attention was given to properly seal the copper tube, to avoid leakages and soil atmosphere contamination by atmospheric components. Moreover sampling soil gas at such a depth considerably lowers risks of sampling gas that could have interact with gas of atmospheric origin. Internal calibration of this sampling method has been done at BRGM (Bureau de Recherches Géologiques et Minières, Orléans, France), reproducibility and results being equivalent to those recorded using stainless steel probes progressively lowered down into the soil by hand-hammer percussion. The copper tube was then connected to the IRGA and pumping done at low flow rate (200 $ml.min^{-1}$). Equilibration of the gas flux occurred within one or two minutes, the time needed to purge all the flexible pipes and then values were registered. Subsequently, two other samples were taken for further analysis. For helium abundance measurements, a Tedlar bag was connected at the exit connection of the IRGA, filled and rinsed prior getting a sample. Last, for radon activity determinations, a vacuumed scintillating flask was filled by soil gas (c.a. 200 ml, internal ZnS coating, Algade, France).

Helium (^4He) measurements were performed twice a day, using a modified Alcatel leaking mass spectrometer (Adixen ASM102S). Values were measured as mV data and then expressed in ppm with reference to the atmospheric value, set to 5.24 ppm. Sensitivity is 0.1 ppm in the range 0.1 ppm – 100 ppm ^4He. Helium measurements were done on a half day basis, samples being analysed less than 4 hours after their collection. The linearity of the spectrometer in the 0.1 – 100 ppm range was checked each time by circulating a 100 ppm reference gas.

Radon measurements (^{222}Rn) were done by alpha particles counting (Calen photomultiplier, Algade) and expressed as activity data (Bq/m^3). Alpha photomultiplier background noise was less than 0.2 counts per hour. Counting was done during 180 seconds, stated reproducibility being better than 0.1%.

If relevant, additional samples were taken in vacuumed glass bulbs for laboratory gaseous chromatography measurements (Varian 3400 gas chromatograph) and further isotope ratio determination by mass spectrometry (Thermo Finnigan Delta S). Gas chromatography was used to determine the proportions of the following gases: CO_2, Ar, O_2, N_2, CO, He, H_2, H_2S, C_nH_{2n+2} (n= 1 to 6). Detection limits are ± 0.0002% for C_nH_{2n+2}, ± 0.001% for Ar, N_2, CO_2, O_2 and ± 0.005% for H_2 and

H_2S. As for the IRGA determination, percentages refer to volume ones. CO_2 isotopic measurements were done on a vacuum purified gas phase after freezing, to get a pure CO_2 fraction. This fraction was then analysed by classical dual inlet mass spectrometer. Stable carbon isotope ratio is expressed as $\delta^{13}C_{CO2}$ with reference to the Vienna Pee Dee Belemnite standard (‰ VPDB). Analytical precision is ± 0.1‰.

3.2 Lake and mineral waters

The Laacher See water mass was investigated in June 2008 in order to characterise the water column and its chemical composition. Water logging was undertaken along an Eastern-Western transect, with some additional data acquisition near the eastern shore where CO_2 escapes were present. Continuous vertical profiling was augmented by *in-situ* spot sampling for chemical and gaseous determinands. Logging was performed using an Idronaut probe (Idro316*Plus*) recording the following parameters: water temperature, pH, redox potential (Eh), conductivity (expressed at 25°C), dissolved oxygen and CO_2 content (expressed as a mV value). Redox data are corrected from temperature influence and expressed with respect to the electro-motive force of the electrochemical reference cell. Water and dissolved gas sampling were performed using a nitrogen driven sampler, samples being taken each 10 m in depth. The stainless steel sampler was slightly over-pressurised (against the hydrostatic pressure existing at the desired sampling depth) at the surface, then gently lowered to the depth of sampling. Once the desired depth was reached, the pressure was slightly lowered to allow the opening of a valve and the filling of the sampler with 1l of water and dissolved species. Then the sampler is re-pressurised and recovered at the surface. Water was then transferred into vacuumed glass bulbs to avoid gas losses.

A set of 20 logs were acquired during the survey. Smaller ones extended up to less than 6 m depth on the Eastern shore and deeper ones up to 48 – 49 m depth in the central part of the lake (figure 1). Depth indicated by the probe may slightly differ from that reported on topographic maps, as “our” depth definition is based on sudden parameter changes induced by lowering the probe into unconsolidated sediments. Moreover, some profiles were performed at constant depth (respectively 1, 4, and 6 m depth) in order to evaluate any lateral discrepancy.

Collected water samples (lake and mineral waters) were analysed at laboratory for major ions by ICP-AES (Inductively Coupled Plasma Atomic Emission Spectroscopy) and chromatographic methods. Dissolved gases were quantified using gas chromatography, using the same methodology as the one used for gaseous species determinations.

3.3 What can be learned from the use of the CO_2 sensor?

Since P_{CO2} sensor are not yet frequently utilised in non-saline water bodies, laboratory testing was performed before in-situ deployment. The P_{CO2} sensor is an adaptation of the Severinghaus electrode (Severinghaus and Bradley, 1958), which consists in a pH determination (expressed as a mV value) using one measuring electrode and one reference electrode, both merged in an electrolyte solution and protected by a gas permeable membrane. Response time should be 30 seconds for a working domain of 0.013 to 0.263 atm CO_2.

First tests were performed by circulating a gas flux of variable CO_2 concentration (0.05 to 100% vol.). The sensor clearly appeared to be better suited for low CO_2 concentrated environments (100 mV of potential difference for a 10% vol. CO_2 range and only 150 mV one for the 0 – 100% vol. range). Moreover the potential difference was time dependent (Figure 2a) therefore correlation of the sensor electrical response with a defined gas concentration is not obvious. At the opposite, sensor behaviour when exposed to different CO_2 concentrations can be used to decipher between progressive enrichment or depletion, depending on the stated electric evolution with time.

Figure 2

(a) Evolution of the electrical response of the CO_2 sensor with time when exposed to progressive CO_2 enrichment (gas phase); (b and c): evaluation of the sensor's equilibration time: (b) when exposed to tap water (low CO_2 content) at time 0 after equilibrating in CO_2-rich water; (c) when exposed to injection of 10% vol. of CO_2 gas in water (starting at time 0).

a

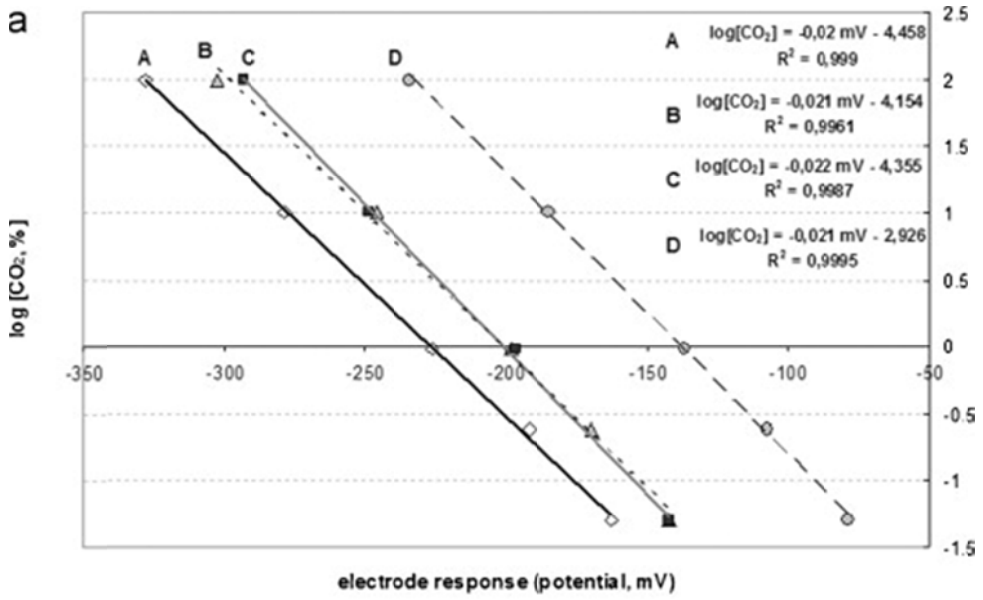
A
B
C
D
A log[CO2] = -0,02 mV - 4,458
R² = 0,999
B log[CO2] = -0,021 mV - 4,154
R² = 0,9961
C log[CO2] = -0,022 mV - 4,355
R² = 0,9987
D log[CO2] = -0,021 mV - 2,926
R² = 0,9995
log [CO2, %]
electrode response (potential, mV)

b

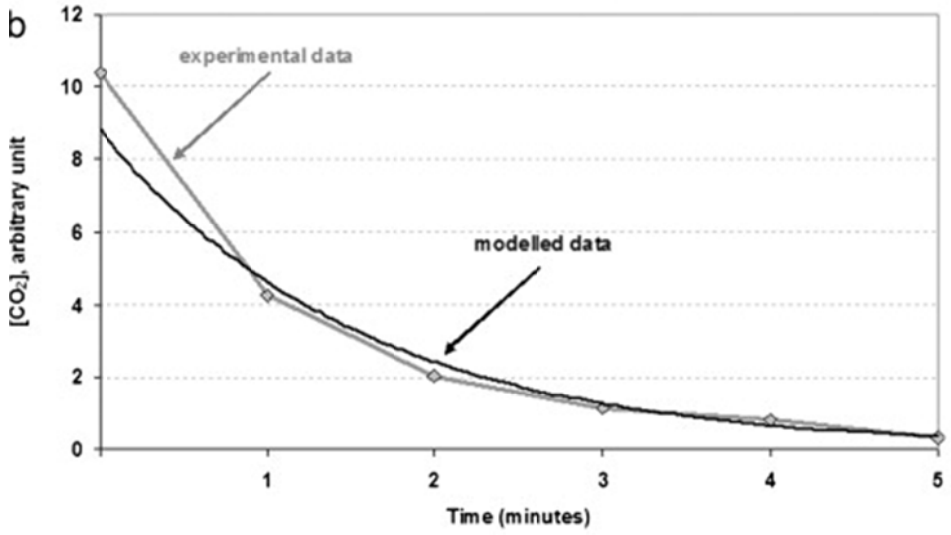
experimental data
modelled data
[CO2], arbitrary unit
Time (minutes)

c

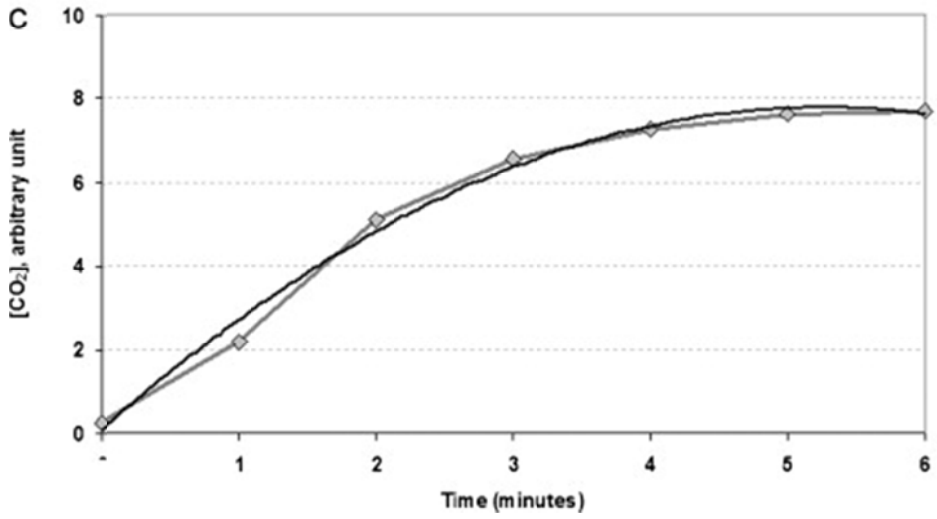
[CO2], arbitrary unit
Time (minutes)

The time needed to achieve equilibrium state in aqueous environment has been evaluated under two schemes: 1) immersion of the probe from CO_2-rich water to tap water (Figure 2b) and 2) injection of a CO_2-rich gas phase in water (Figure 2c). The electrical potential evolved exponentially with time for case 1 and under polynomial regression for case 2. Time needed to reach 80% of the ending electrical signal was close to 2 minutes for CO_2 loss (case 1) and close to 3 minutes for CO_2 enrichment (case 2). This quicker time reaction for decreasing CO_2 concentrations than for increasing ones is conflicting with previous studies (Severinghaus and Bradley, 1958). Moreover, its implies to perform logging (probe deepening) at slow speed, typically between 0.5 to 2 m per minute in order to detect variations at a metric scale.

The evolution of the sensor response with temperature, that may induce variations of the CO_2 dissolved content (Diamond and Akinfiev, 2003), has been tested at 11 and 15°C, suggesting a lesser amount of dissolved CO_2 at higher temperature in agreement with calculated parameters based on gas saturated solution.

An in-situ test was conducted in the French Massif Central (Détente well; Renac *et al.*, 2009). This 560 m deep well has been surveyed up to 400 m depth in order to explore both the two phase part (coexistence of dissolved and gaseous CO_2, from 0 to 115 m depth) and the deeper part (below 115 m depth) where only dissolved CO_2 is present (Iundt and Robalo, 1990). Probe deepening was lesser than 2.4 m per minute in the 0 – 115 m depth interval and not larger than 5.1 m per minute downwards. Some stops were also made during lowering (Figure 3).

Stability of measurements was lesser in the two phase part of the well than in the deeper part, where no drift occurred when performing stops during probe lowering. Below 115 m depth, the mV evolution suggested a progressive enrichment in dissolved gas that was consistent with laboratory gas analyses (from 0.026 to 0.27 mol/l at depth) and with partial CO_2 pressures calculated from water chemistry (from 1.2 at surface to 12.8 atm at 260 m depth). There was no redhibitory instrumental drift with time. If we postulate that pH is mainly influenced by the CO_2 content, evolution of CO_2 data along with these pH data also suggested a consistent evolution, the progressive diminution of the pH value being more or less linked to enrichment in dissolved CO_2, especially below 250 m depth. Some discrepancies did exist between 115 and 250 m depth, as the CO_2 sensor suggested the existence of a less rich horizon. Dissolved CO_2 amounts and potential values from the CO_2 sensor were linked as follow:

$[DCO_2] = 44 \exp [-0.0658 A – 21.08]$; $r^2 = 0.993$; $n = 5$ (1)

with $[DCO_2]$ the dissolved CO_2 concentration in mg/l and A the read of the CO_2 sensor in mV.

Even if this preliminary in-situ testing was performed in CO_2–rich water, it has shown that the CO_2 sensor can help in evaluating the relative quantities of dissolved gas, variations due to temperature and time being of secondary importance. Nevertheless no quantification of the dissolved amount appeared to be realistic (Figures 2 and 3).

Figure 3

Water logging of Détente well: plot vs. depth of water temperature, pH and CO_2 (as mV value); dashes along the depth axis figure the depths where stops were made during logging. Lower right graphs represent the variation of the CO_2 value as a function of water temperature and logging duration.

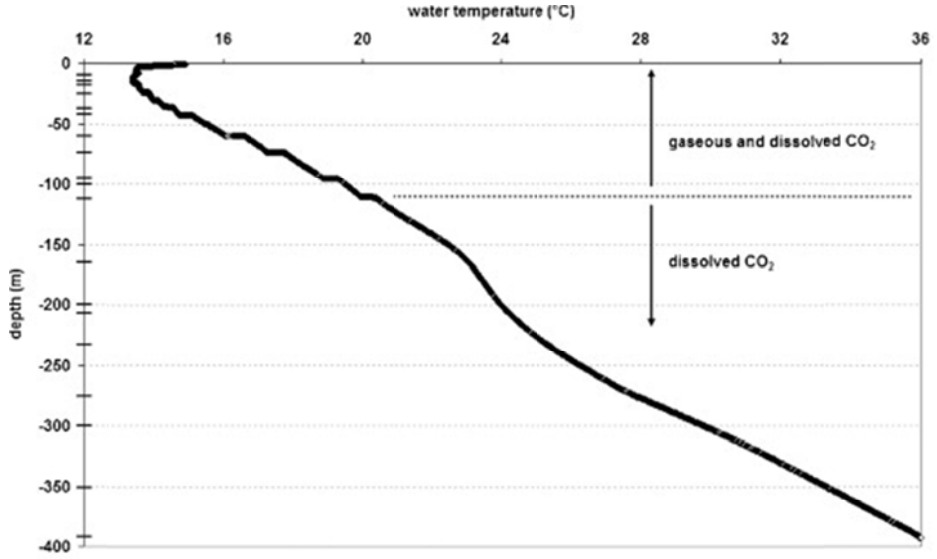
water temperature (°C)
12
16
20
24
28
32
36
depth (m)
0
-50
-100
-150
-200
-250
-300
-350
-400
gaseous and dissolved CO_2
dissolved CO_2

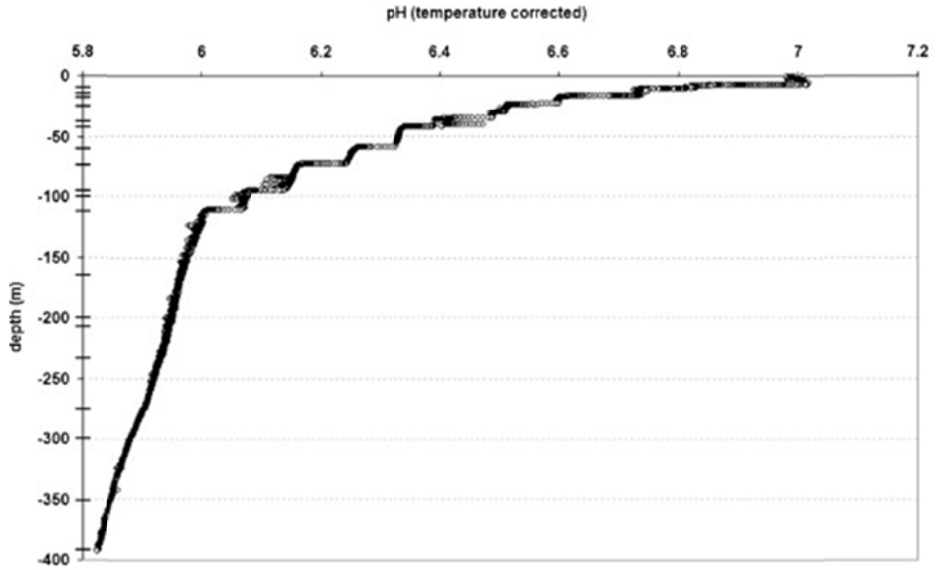
pH (temperature corrected)
5.8
6
6.2
6.4
6.6
6.8
7
7.2
depth (m)
0
-50
-100
-150
-200
-250
-300
-350
-400

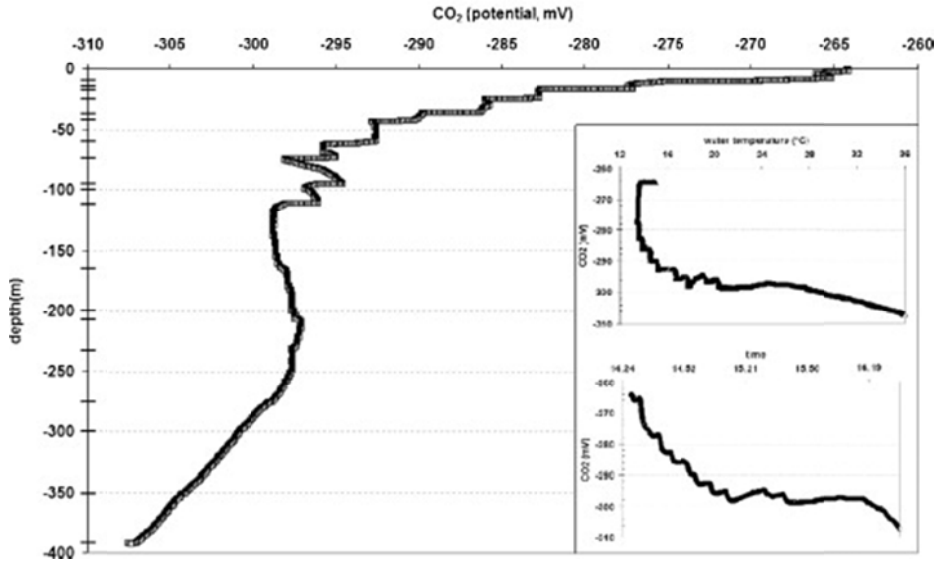
CO_2 (potential, mV)
-310
-305
-300
-295
-290
-285
-280
-275
-270
-265
-260
depth(m)
0
-50
-100
-150
-200
-250
-300
-350
-400
water temperature (°C)
time

4. Soil gas data

4.1 External forcing

Even if this study was focussed on soil gas studies in the vicinity of gas vents (mofettes where an input of deep CO_2 is present), gas migration in near surface processes always depends on meteorological conditions (Toutain and Baubron, 1999). In order to get an overview of the main meteorological parameters before the September 2007 soil gas survey, we get daily means of these parameters from the Koblenz-Bendorf weather station, located 20 km ESE from Laacher See lake at 130 m a.s.l.

Figure 4 Meteorological parameters (air temperature, rainfall amount, barometric pressure, sunshine duration and relative humidity) before and during the survey; data from Koblenz–Bendorf weather station, http://www.weatheronline.co.uk/.

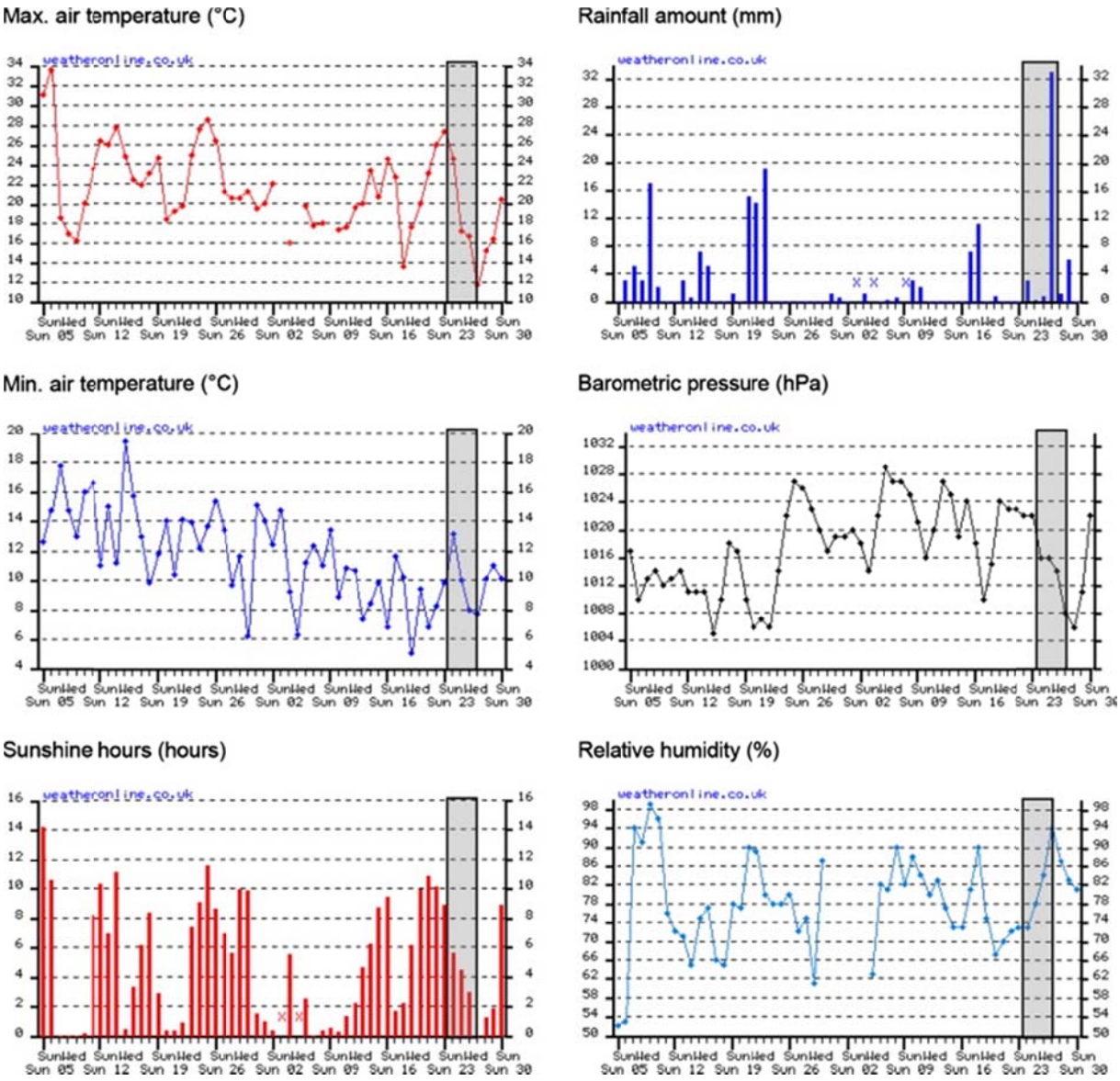

During the survey itself (24^{th} – 27^{th} of September 2007), atmospheric temperature experienced a sharp decrease, from 24 to 12°C for maximum ones and from 13 to 8°C for minimum ones. This was the consequence of the existence of a low pressure barometric system (1016 to 1008 hPa) that led to a great reduction of sunshine duration (from 6 hours on to 0), consequent rainfall amounts (3 mm on day 24, 33 mm on day 27) and a rise in relative humidity levels (from 73% to 94%).
During the weeks preceding the survey, air temperatures experienced a decrease directly linked to seasonal variation, from summer to autumn conditions. Rainfall amounts were low between end August to mid-September (less than 30 mm). As a consequence sunshine duration and barometric pressures exhibit quite high values, with relative humidity varying together with precipitations.

Radon contents in soils are dependent from those meteorological parameters (Finkelstein *et al.*, 1998), as well as other gases such as CO_2 (Heinicke *et al.*,1993) or helium (Virk and Walia, 2001). Radon concentrations are *e.g.* dependent from diurnal variation linked to the sun rise on the morning, which is related to air temperature; from the possible partial dissolution of the gas into percolating water when raining; from changes due to barometric pressure fluctuations; from the effect of winds and ventilation.
Quantification of diurnal variations of gas contents within soils is not achievable as measurements were performed only once for a selected point. Barometric pressure variations are small (8 hPa) and their effect at one meter depth should be very low. Temperature variations are abrupt in the atmosphere (Figure 4), but similarly at depth they are likely to be attenuated and delayed. Soil humidity levels could be more variable as rainfalls occur at the end of the survey. Nevertheless, large amounts of rainwater are needed to modify soil gas concentrations (Wattananikorn *et al.*, 1998). With regard to the meteorological evolution from August to September 2007, sudden changes on soil water content can be discarded for the Laacher See site and can only have influenced upper soil gas concentrations at the Obermendig site, where sampling was done during a 33 mm rainfall event.

Thus changes stated on soil gas concentrations must preferentially reflect heterogeneities linked to soil or tectonic structures affecting underlying rocks (Baubron *et al.*, 2002; Ciotoli *et al.*, 1999). In that sense measurements appear to be more related to the characterization of the geological framework rather than to rely on externally driven variations. Moreover, the Laacher See district is a nowadays

non-active area as no residual volcanic nor great tectonic activity is experienced, but it can neither be viewed as a pure non active area as gas fluxes from depth still occur, as highlighted by acquired data. Gas emanation should then be controlled by advection processes rather than by diffusion processes. Figure 5 favours this statement, as no correlation with meteorological evolutions was highlighted. Furthermore, soil gas data acquired away from areas with deep degassing would exhibit an opposite behaviour. For example, radon activities sometimes decline when atmospheric temperatures do or when barometric pressures rise (Kumar *et al.*, 2009).

Figure 5

Plot of soil gas measurements vs. time of sampling.

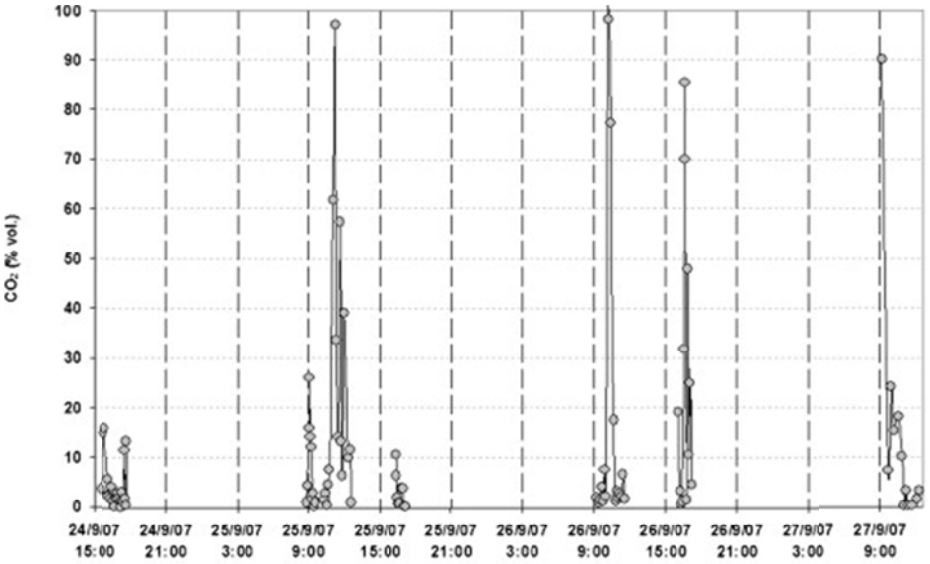
CO_2 (% vol.)
100
90
80
70
60
50
40
30
20
10
0
24/9/07 15:00
24/9/07 21:00
25/9/07 3:00
25/9/07 9:00
25/9/07 15:00
25/9/07 21:00
26/9/07 3:00
26/9/07 9:00
26/9/07 15:00
26/9/07 21:00
27/9/07 3:00
27/9/07 9:00

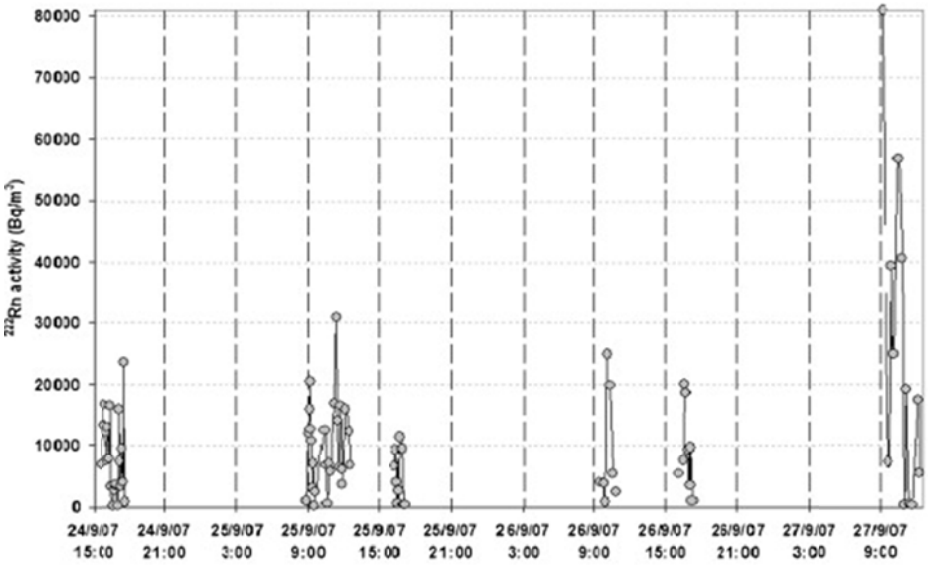
^{222}Rn activity (Bq/m^3)
80000
70000
60000
50000
40000
30000
20000
10000
0
24/9/07 15:00
24/9/07 21:00
25/9/07 3:00
25/9/07 9:00
25/9/07 15:00
25/9/07 21:00
26/9/07 3:00
26/9/07 9:00
26/9/07 15:00
26/9/07 21:00
27/9/07 3:00
27/9/07 9:00

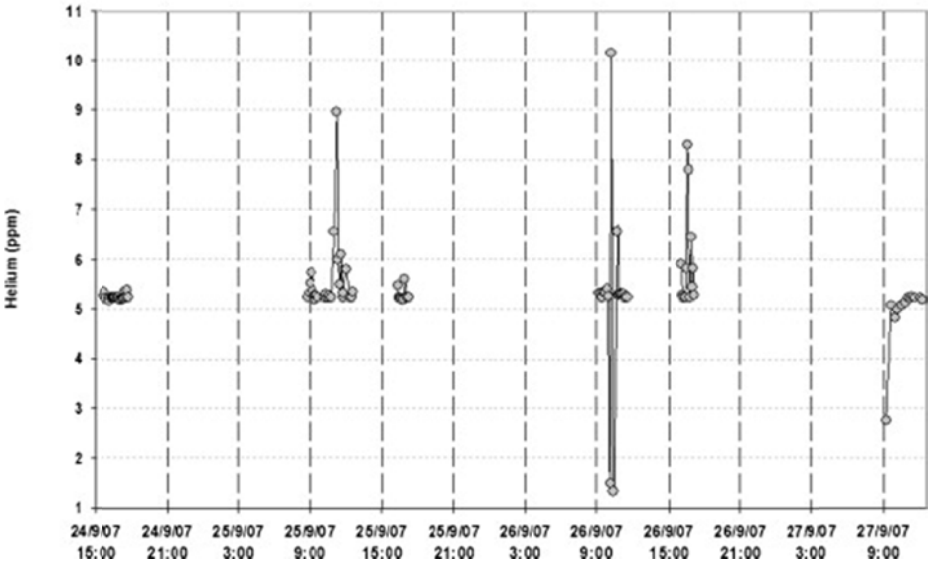
Helium (ppm)
11
10
9
8
7
6
5
4
3
2
1
24/9/07 15:00
24/9/07 21:00
25/9/07 3:00
25/9/07 9:00
25/9/07 15:00
25/9/07 21:00
26/9/07 3:00
26/9/07 9:00
26/9/07 15:00
26/9/07 21:00
27/9/07 3:00
27/9/07 9:00

4.2 Results and Interpretation

CO_2 concentrations on the western shore of the Laacher See (sampling between the 25th and the 26th of September) ranged between atmospheric values (0.03%) to 100% vol. They were associated with ^{222}Rn activities from 120 to 30800 Bq/m^3. Respective mean values were 13.8% and 8630 Bq/m^3 (Table 1). Helium-4 concentrations plotted in a wide range, between 1.3 and 10.1 ppm, with a mean value slightly enriched relative to the atmospheric level. Such a helium distribution had a wider variability than reported for other leaking sites, *e.g.* Latera caldera in Italy (Beaubien *et al.*, 2008), where concentrations lesser than 4 ppm were not monitored. Some additional measurements (Table 1) performed 5 km to the Southwest (Obermendig site), near the Erlenbrunnen mineral spring, revealed higher radon activities, similar CO_2 concentrations and confirmed the existence of negative helium anomalies (amounts lesser than the atmospheric value). No CH_4 was detected by the IRGA in the field.

Table 1

Soil gas measurements statistics: (a) Laacher See site; (b) Obermendig site.

a)	^{222}Rn (Bq/m^3)	CO_2 (%)	O_2 (%)	^4He (ppm)
Number of observations	70	87	87	87
Minimum	120	0,03	0	1,33
Maximum	30800	100	20,6	10,1
Median	6960	3,3	18,9	5,25
Mean	8630	13,8	17,2	5,44
Standard deviation	6840	23,7	4,5	1
Coefficient of variation	0,793	1,722	0,262	0,185

b)	^{222}Rn (Bq/m^3)	CO_2 (%)	O_2 (%)	^4He (ppm)
Number of observations	12	12	12	12
Minimum	330	0,13	3,5	2,75
Maximum	81000	90	20,3	5,26
Median	18300	5,3	19	5,16
Mean	24500	14,5	17,2	4,93
Standard deviation	24500	24	4,5	0,67
Coefficient of variation	0,999	1,664	0,261	0,136

Spatial distribution of CO_2 and radon on the western shore of Lake Laacher See are presented in Figure 6. Data interpolation was done using the natural neighbour algorithm as no well-defined variogram could be built to perform reliable krigging. This natural neighbour plot highlights the occurrence of a very emissive zone (gas vent) on the southern part of the monitored area (near points B and C) that is evidenced by high CO_2 contents and pronounced radon activities compared to

adjacent values. Another high gas content zone can be evidenced in the Northern part of the meadow. Decreasing of the CO_2 content back to non-anomalous values is done in a 20 m distance interval, close to spacing stated in Italy by Beaubien *et al.* (2008) if referring to their background value definition (concentrations lesser than 2.5% vol. CO_2). Here we prefer using another commonly used approach (Xue *et al.*, 2008). An anomalous level was here defined by the "mean plus twice the standard deviation" parameter. For the Laacher See pasture, the thresholds were respectively 61.2% vol. for CO_2, 22,300 Bq/m^3 for ^{222}Rn and 7.44 ppm for ^{4}He. Interestingly, frequency distribution histograms (Baubron *et al.*, 2002) yielded to similar results, 93.1% of the CO_2 values being under 66% vol., 95.7% of the ^{222}Rn values being under 21,700 Bq/m^3 and 95.4% of the ^{4}He values being under 7.44 ppm. Last, as often stated for soil gases, the CO_2 concentrations were ranged under log-normal distribution (probability of 94.3%), but both ^{222}Rn and ^{4}He were not, neither they were under normal distribution.

Only seven samples had a CO_2 concentration greater than 61%, lying between points B and C (Figure 6); by them 4 points also had anomalous helium content, and only one showed a conjoint CO_2-He-Rn anomaly. Two other samples had great radon activities without particular concentration in other gas species. Using such an approach may help to refine the definition of anomalies, i.e. there is only one true gas vent existing in the monitored area. Specifically, radon activities reaching values up to 20,000 Bq/m^3 on the northern part of the surveyed area did not seem to be related to the existence of an active gas vent, even if CO_2 concentrations do reach few tens of % vol.

The contrasting behaviour of the ^{4}He gas (Figure 6), with either enrichment or depletion relative to the atmospheric level, could then be interpreted as follow: the active centre of the vent allows the conjoint escape of both carbon dioxide and helium. As helium is co-eluted with other gases under great fluxes (> 500 g/m^2/day for this vent; Jones, 2009, pers. comm.) and has a lower density than the air, it is drained out by the other gaseous species. As a consequence, soil formations existing close to the vent exhibit very low helium concentrations, that progressively come back to near atmospheric levels when moving away from the vent. Narrower helium anomalies compared to CO_2 ones were also stated in Italy (Beaubien *et al.*, 2008). Helium originated from decaying of uranium-rich formations (Etiope and Martinelli, 2002) and at the opposite uranium-poor levels does not seem to be a valuable explanation, as spatial variations are too narrow and radon activities too small. Testing this hypothesis could be done in the future by performing helium isotope measurements ($^{3/4}$He ratio). As helium in the Laacher

See region is mainly of mantle origin (Aeschbach-Hertig *et al.*, 1996, 1999), this pumping effect could be also evidenced by isotope ratios that would show a progressive rise of atmospheric component together with increasing distance from the vent.

Figure 6

Soil gas species along the western shore of lake Laacher See. Interpolation is done using natural neighbour computation, and is only valid near the set of 86 measurements (location represented by dots on central inset). Location of the western shoreline of the lake is indicated. Grid scaling: 20 m interval.

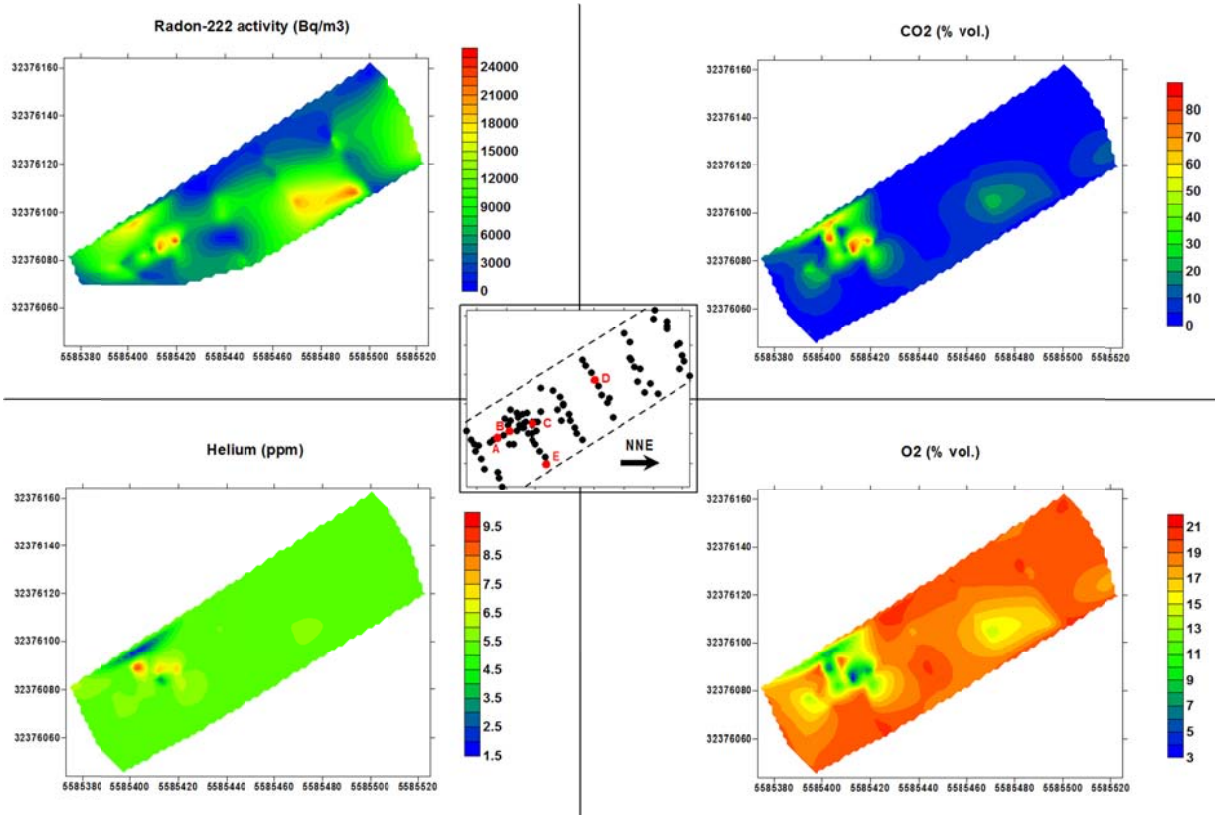

As a consequence of gas venting, there is a strong negative correlation between O_2 and CO_2 contents (Table 2), that could be explained by a progressive replacement of O_2 by CO_2 as the CO_2 concentration increases. The centre of the vent is then almost anoxic. There is also a slight correlation between ^{222}Rn and CO_2. In this case, CO_2 could act as a carrier gas, allowing ^{222}Rn transportation along its migration pathways (Heinicke *et al.*, 1993). Nevertheless the depth where radon originates cannot be postulated, as it depends on the migration speed of the other mobile gases and on the soil physical parameters, which are different from one site to another.

Table 2

Correlation matrix—all data (Pearson coefficient).

	^{222}Rn (Bq.m^{-3})	CO_2 (%)	O_2 (%)	^{4}He (ppm)
^{222}Rn (Bq.m^{-3})	**1**			
CO_2 (%)	0,579	**1**		
O_2 (%)	-0,596	-0,991	**1**	
^{4}He (ppm)	-0,165	0,047	-0,04	**1**

Such soil gas concentrations, especially those for CO_2 and ^{4}He, are characteristic of emissive areas, similar to those known in the French Massif Central (Battani *et al.*, 2010) or in Italy (Beaubien *et al.*, 2008). Helium concentrations are nevertheless diluted regarding concentrations found in gas bubbles within the Laacher See itself (up to 20 ppm; Aeschbach-Hertig *et al.*, 1996), whereas radon activities in France or Italy are much higher (up to thousands of kBq/m^3). This is could be attributed to different soils characteristics and to different basement geology. Those measurements might prove one of these effects linked to different soil structures. As said before, the Laacher See site is exposed to the atmosphere only since hundreds of years. Structures and organics layers inherited from underwater stage are still to be found within this soil (Krüger *et al.*, 2009), while soils at Obermendig (sampling on the 27th of September) have never been affected by such an evolution. Therefore this could partly result in observing similar carbon dioxide contents, especially above gas vents, but different radon levels.

Gas chromatography results revealed a good agreement between in-situ measurements and laboratory analyses (Table 3). Linear regression computations done on CO_2 and O_2 results lead to correlation's coefficients of 0.992 and 0.991 respectively, IRGA measurements slightly overestimating laboratory ones. This could be an effect of the time delay needed to bring back samples to laboratory, as it's especially noticeable for the high content samples. Other ubiquitous gaseous species were argon, with levels slightly lower than the atmospheric mean (0.93) and nitrogen. Two samples (D and E in Figure 6) had noticeable methane content (29 and 150 ppm respectively) that was well above atmospheric level (1.7 ppm). This enrichment could be the result of gas release together with CO_2 of deep origin. Beaubien *et al.* (2008) have noticed such methane enrichment in areas where CO_2 flux is greater than 500 g/m^2/day, methane oxidation processes becoming lesser noticeable. Methane enrichment was found in samples far away from the gas vent, preferably being the result of bacterial

activity in soils (methanotrophic species). Unfortunately, since none $\delta^{13}C_{CH4}$ measurement was performed, deciphering between those two hypotheses is not possible.

Table 3

Gas chromatography results; samples location is indicated in Fig. 3; d.l.: detection limit; precision of isotope ratio measurements is ±0.15‰ VPDB.

	Ar	N_2	CO_2	*$CO_{2,\ IRGA}$*	O_2	*$O_{2,\ IRGA}$*	He – H_2 – H_2S	CH_4	$C_nH_{2n+2,\ n=2\ to\ 6}$	$\delta^{13}C$ (‰ VPDB)
d.l.	*0,001*	*0,001*	*0,001*		*0,001*		*0,005*	*0,0002*	*0,0002*	
Pt. A	0,55	47,2	39	*39,2*	12,5	*12,3*	< d.l.	< d.l.	< d.l.	-1,9
Pt. B	0,87	73,3	5,75	*6,38*	19,5	*19,1*	< d.l.	< d.l.	< d.l.	-1,5
Pt. C	0,41	36,7	52,2	*61,6*	9,75	*7,9*	< d.l.	< d.l.	< d.l.	-4,1
Pt. D	0,8	68,1	13,3	*14*	17,7	*16,8*	< d.l.	0,0029	< d.l.	-2,6
Pt. E	0,32	24,4	67,4	*77,5*	6,63	*5,5*	< d.l.	0,015	< d.l.	-2,6

Laboratory results pointed out a dominant deep origin for the CO_2 gas and argon concentrations suggesting a greater proportion of the deep gas flux. This deep origin was also indicated by carbon isotope ratio measurements. Ratios between -1.5 to -4.1‰ VDPB were measured (Table 3; mean value: -2.5‰) that agree well with those reported elsewhere for the CO_2 escapes within the lake (-3.7 to -3.8‰ in Giggenbach *et al.*, 1991; -3‰ in Griesshaber *et al.*, 1992). The more negative ratios seem to be linked to a "deep origin" component (mantle and/or crustal degassing), also highlighted in non-emissive areas (Pauwels *et al.*, 2007) and are clearly not related to interaction with CO_2 produced by biological phenomena. Less negative ratios can perhaps be related to interaction within soil formations, *e.g.* with carbonate horizons.

5. Lake Laacher See and mineral springs

5.1 Chemical composition of Erlenbrunnen mineral spring and lake waters

Chemical composition of the Erlenbrunnen spring reflected the mean composition of mineral waters of the Eifel district (Griesshaber *et al.*, 1992; van der Bogaard, 1995). This spring had a low discharge temperature (11.6°C), a Total Dissolved Solids (TDS) amount lesser than 4000 mg/l, high free CO_2 gas content (calculated pCO_2 = 1.13 atm), a slightly acidic pH and was of Ca-Mg-HCO_3 type (respective concentrations of 305, 220 and 3800 mg/l). Chlorine content was less than 10 mg/l (Figure

7, Table 4). Carbonate system was dominated by the H_2CO_3/HCO_3 couple. Erlenbrunnen water appeared to be slightly oversaturated with respect to Ca-CO_3 species (calcite, aragonite, dolomite) and slightly undersaturated with respect to Ca-SO_4 ones (anhydrite, gypsum). As a consequence, this spring will be considered as representative of the deep end-member even if local mineral waters are frequently mixture between old and young groundwaters (van der Bogaard, 1995).

Figure 7

Schöeller–Berkaloff diagram showing major ion contents of Erlenbrunnen mineral spring and Laacher See (LS) lake from near surface (−1.7 m) to bottom (−46 m); surface and bottom characteristics of Lake Pavin water (French Massif Central) are also indicated for comparison (BRGM, 2009, unpublished data).

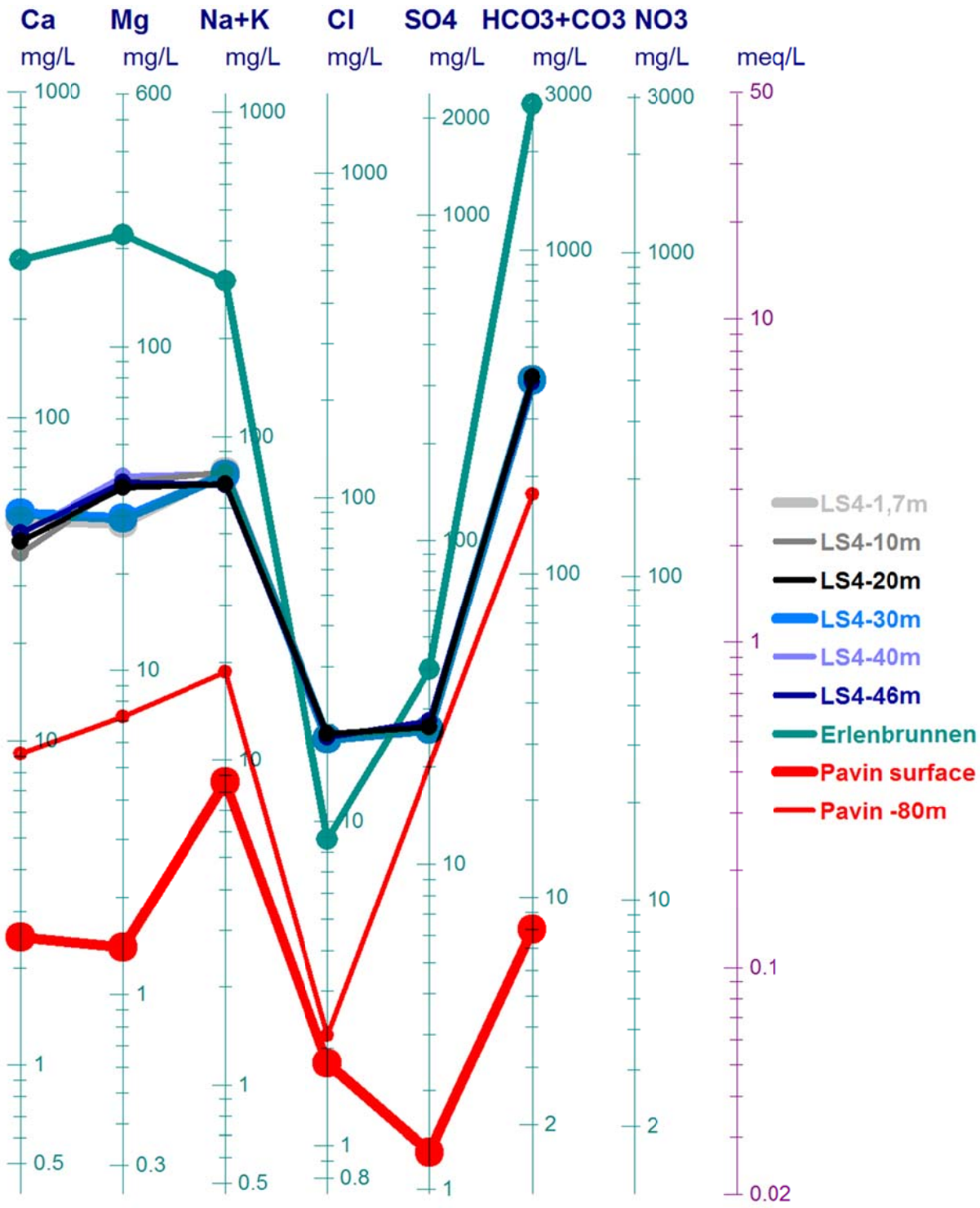

Table 4

Chemical analyses of Laacher See water and Erlenbrunnen mineral spring; chemical balances are in the range −2 to +4%. For samples LSX refer to Fig. 1 for location; sampling depth is indicated after the hyphen. Saturation index (SI) and mmol/l concentrations of carbonated species (TDIC = Total Dissolved Inorganic Carbon = H_2CO_3 + HCO_3 + CO_3) are computed using Diagramme software (http://www.lha.univ-avignon.fr/LHA-Logiciels).

Sample	TDS (mg/l)	T (°C)	pH	Cond. @25°C (µS/cm)	Ca (mg/l)	Mg (mg/l)	Na (mg/l)	K (mg/l)	HCO_3 (mg/l)	Cl (mg/l)	SO_4 (mg/l)	F (mg/l)
LS5 bubbles	581	24,8	8,11	657	41,3	38,4	46,4	24,7	384,9	18,5	26,3	0,56
LS5-20cm	592	27,4	8,26	643	49,7	28	45,7	30,6	392,8	18	26,4	0,54
LS4-1.7m	598	20,4	8,45	655	47,8	28,5	48,6	29,1	398,9	18	26	0,55
LS5-2m	592	20,5	8,26	654	44,6	38,1	49,3	22,9	392,2	18,3	26,2	0,55
LS4-10m	601	8,2	8,12	665	37,9	38	51,1	26,5	402,6	18,4	26,3	0,56
LS4-20m	601	5,6	7,8	659	41,1	36,8	46,6	25	405,7	18,7	26,4	0,57
LS3-30m	614	5,2	7,77	653	46,4	39,5	48,7	25,2	408,7	17,9	26,9	0,55
LS4-30m	595	5,2	7,55	666	50,4	29,5	48,2	28	394,7	18,1	25,9	0,55
LS4-40m	606	5,1	7,45	663	43,5	39,8	50,3	26,6	400,8	18,4	26	0,57
LS2-45m	603	5	7,35	617	50,4	24,8	47,4	29,4	406,3	18,1	25,8	0,56
LS4-46m	590	5	7,15	680	44	38,1	48,5	22,3	390,2	18,1	27,8	0,55
Mean	*597,5*	*12*	*7,8*	*655,6*	*45,2*	*34,5*	*48,2*	*26,4*	*398*	*18,2*	*26,4*	*0,56*
Std. Dev.	*8,91*	*9,15*	*0,43*	*15,87*	*4,15*	*5,55*	*1,64*	*2,68*	*7,58*	*0,23*	*0,56*	*0,01*
Mean / SD	*1,50%*	*76%*	*5,50%*	*2,40%*	*9,20%*	*16,10%*	*3,40%*	*10,10%*	*1,90%*	*1,30%*	*2,10%*	*1,40%*
Erlenbrunnen	3686	11,6	6,35	3100	305	221	234	67,9	2808,4	8,8	40	0,44

Sample	$SI_{Calcite}$	$SI_{Aragonite}$	$SI_{Dolomite}$	SI_{Gypsum}	$SI_{Anhydrite}$	TDIC (mmol/l)	H_2CO_3 (mmol/l)	HCO_3 (mmol/l)	CO_3 (mmol/l)	pCO_2 (atm)
LS5 bubbles	0,86	0,71	1,48	-2,27	-2,49	6,38	0,109	6,233	0,038	0,003
LS5-20cm	1,14	1	1,87	-2,18	-2,39	6,458	0,076	6,325	0,057	0,002
LS4-1.7m	1,21	1,06	1,92	-2,22	-2,45	6,516	0,054	6,385	0,076	0,001
LS5-2m	0,98	0,83	1,61	-2,25	-2,48	6,462	0,083	6,33	0,049	0,002
LS4-10m	0,58	0,42	0,62	-2,32	-2,58	6,722	0,15	6,545	0,027	0,003
LS4-20m	0,25	0,09	-0,15	-2,28	-2,54	6,976	0,339	6,624	0,012	0,005
LS3-30m	0,26	0,1	-0,15	-2,23	-2,48	7,057	0,37	6,676	0,011	0,006
LS4-30m	0,07	-0,09	-0,7	-2,2	-2,46	7,056	0,594	6,455	0,006	0,009
LS4-40m	-0,1	-0,26	-0,84	-2,27	-2,52	7,325	0,762	6,558	0,005	0,012
LS2-45m	-0,12	-0,28	-1,16	-2,2	-2,45	7,629	0,975	6,65	0,004	0,015
LS4-46m	-0,4	-0,56	-1,48	-2,23	-2,49	7,878	1,485	6,39	0,003	0,023
Erlenbrunnen	0,39	0,23	0,19	-1,5	-1,76	103,72	57,69	46,02	0,004	1,132

Equations used for computing the chemical equilibrium of the carbonate system:

K_0, equilibrium constant of the reaction: $H_2O + CO_2 <=> H_2CO_3$ $K_0 = \frac{[H_2CO_3]}{P_{CO2}}$

K_1, equilibrium constant of the reaction: $H_2O + H_2CO_3 <=> H_3O^+ + HCO_3^-$ $K_1 = \frac{[HCO_3^-] * [H_3O^+]}{[H_2CO_3]}$

K_2, equilibrium constant of the reaction: $H_2O + HCO_3^- <=> H_3O^+ + CO_3^{2-}$ $K_2 = \frac{[CO_3^{2-}]}{[HCO_3^-]}$

$\log K = A + B * T + \frac{C}{T} + D * \log T + \frac{E}{T^2}$ A, B, C, D and E constants taken from PhreeQC database

Laacher See waters had relatively high TDS contents (*c.a.* 600 mg/l) compared to those of *e.g.* Lake Pavin (Figure 7), set in a similar geological context (Aeschbach-Hertig *et al.*, 1999), where TDS contents only reach 400 mg/l at lake's bottom (BRGM, 2009, unpublished data). There were no significant TDS variations along the water column in Laacher See waters, dominant species being HCO_3, Ca and Mg as for mineral waters (Table 4). Chlorine contents reached twice the value of the Erlenbrunnen spring and were almost constant throughout the water column as well as other anions contents (variations lesser than 2.1% of the mean / standard deviation ratio). Changes were greater

for cationic species, variations of 10% or more existing for Ca, K and especially Mg. As a consequence saturation indexes did vary with depth, waters being oversaturated with respect to Ca carbonated species at surface horizons and progressively becoming undersaturated with depth. Saturation changes appeared between 20 and 40 m depth (Table 4), in agreement with reported changes of sediment facies (Bahrig, 1985). The carbonate system was mainly governed by the bicarbonate specie which accounted for c.a. 98% of the Total Dissolved Inorganic Carbon (TDIC) from 0 to 10 m depth in, 90 to 95% from 20 to 45 m depth and c.a. 80% at the interface with unconsolidated sediments. Calculated CO_2 partial pressures were 2 to 3 orders of magnitude lesser than for the Erlenbrunnen spring, maximum pressure (0.023 atm) being reached at maximum depth. Similar values are only obtained under the chemocline barrier within Lake Pavin (Aeschbach-Hertig *et al.*, 1999), suggesting a substantial enrichment of Laacher See waters, with respect to TDS values.

One intriguing point is the ubiquitous chlorine richness of the Laacher See waters. Lake waters appear to have contents similar to or greater than the majority of the neighbour mineral waters (Griesshaber *et al.*, 1992). Chlorine content coming from rainwater can only reach few ppm even in near coastal environments (Koehler and Wassenaar, 2010). Chlorine coming from water/rock interactions in near surface environments is not believed to be an important supplier, as the Eifel district is not known for peculiar Cl-rich rock formations. Moreover in such a case water type should have been modified (*e.g.* rising of the Na or K concentrations) which is not identifiable, Na+K concentrations being lesser than those of mineral waters. Chlorine richness is not reported in crater lakes where CO_2 is known to accumulate, *e.g.* Lake Nyos (less than 1 mg/l; Giggenbach, 1990). Another option could be an input of gaseous chlorine, considerable amounts being reported in some volcanic districts (*e.g.* 800 to 7500 ppm in magmas; Aiuppa *et al.*, 2009). However, the exsolution of chlorine (as HCl) is frequently concomitant with those of CO_2, and hence such an origin would also be characterised by strong CO_2 amounts. Excepted some onshore and offshore gas vents, there is no evidence of a strong and generalised degassing in the Eifel region. Moreover the gas phase measured on mofettes is mainly CO_2 (99 to 100% vol.) and chlorine abundances in the Eifel groundwaters is also consequently lesser than the one of CO_2 (resp. 0.3 – 0.6 and 55 – 60 kmol/l; Griesshaber *et al.*, 1992).

If a dominant Cl origin from degassing can be discarded, Laacher See water enrichment towards local groundwaters remains unexplained. Surface water feeding of the lake, either by rain waters or streams, should not be the only purveyor. As suggested for Lake Pavin (Jézéquel *et al.*, 2009),

underwater seepages of mineral waters, possibly of different chemical characteristics, may be one of the options to explain the peculiar chemical content of Laacher See waters. Complementary isotope analyses in the future may help to evaluate this hypothesis.

5.2 Lake water logging

Chemical data resulting from in-situ sampling were completed by diagraphies as described in section 3.2. Results are presented in Figures 8 to 10. Temperature and conductivity changes are expected to be linked to the physical characteristics of the lake body, and dissolved oxygen, pH and redox variations to be impacted by biological processes in this meso- to eutrophic lake.

Figure 8 is based on data acquired in the centre of the lake (see Figure 1), 200 m southward from the zone where measurements were performed by Aeschbach-Hertig *et al.* (1996). Temperature data were in good agreement with these previous data. Discrepancies that existed between 0 and 20 m depth could be attributed to the holomictic character of the lake. Since measurements were made in late June, waters have warmed during spring time but did not reach their thermal optimum that is frequently observed at the end of the summer time. There was a strong decreasing thermal gradient between 5 and 15 m depth (thermocline) all over the lake (Figure 9a), with some slight lateral heterogeneity that was probably related to non homogeneous mixing within the epilimnion. At 20 m depth 5.4 to 5.6 °C were reached, followed by a small temperature decrease in the hypolimnion, where 5°C represented the ubiquitous temperature. This bottom temperature was higher than the one reported by Aeschbach-Hertig *et al.* (1996) who gave a 4.3 – 4.5°C range, even if they found a slight warming in the last 5 m. As we found this 5°C value several times, we do think it reflected the real bottom temperature, suggesting a better vertical homogenisation during this 2008 spring than previously noticed.

Figure 8

Synthetic view of deepest logs acquired in the Laacher See. Labels in captions refer to Fig. 1. Data from May and September months are from Aeschbach-Hertig et al. (1996). The inset in O_2 vs. depth diagram shows the relationship between O_2 and pH.

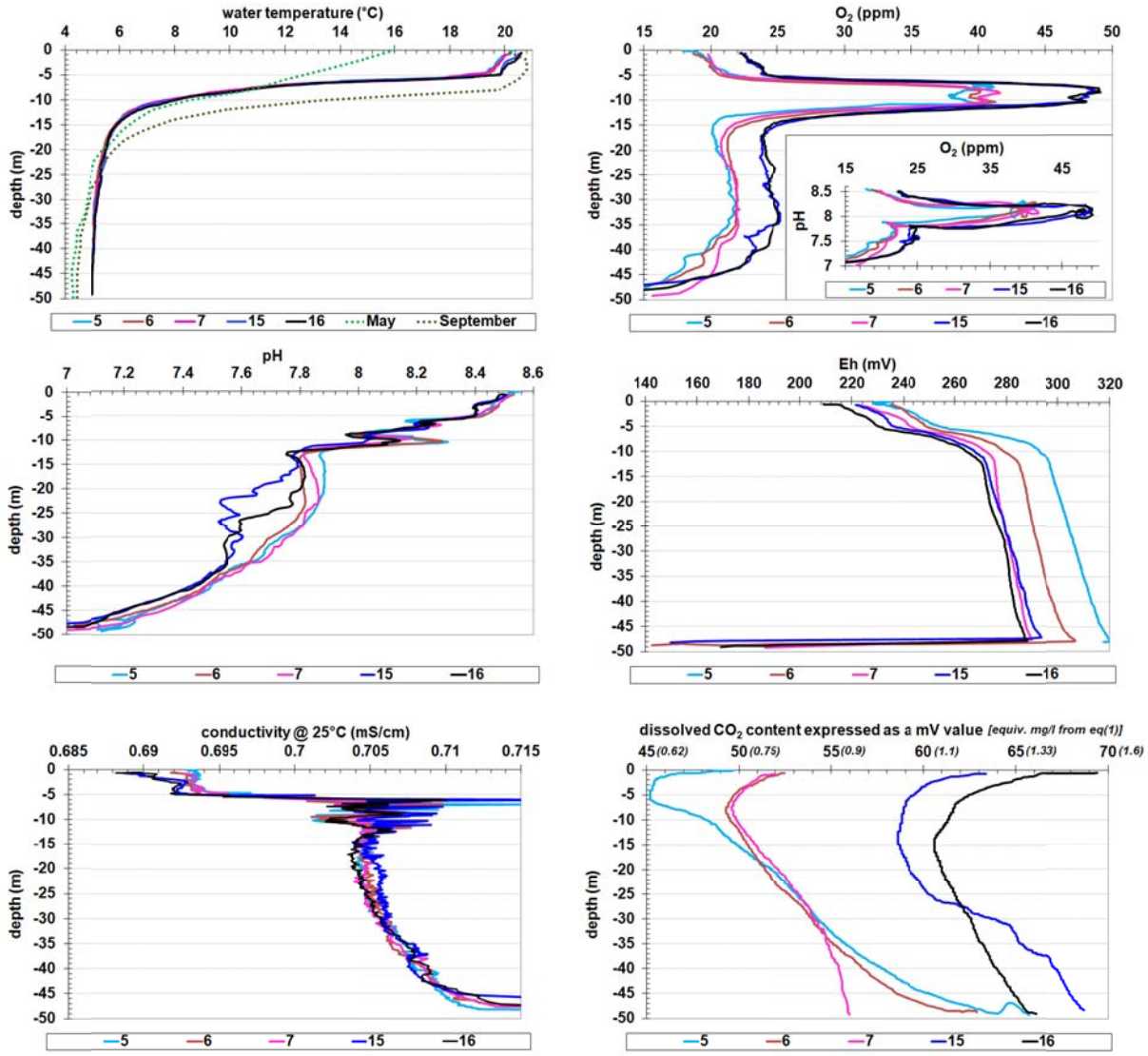

Figures 9a and 9b

(a) Interpolation map drawn using the natural neighbour algorithm:evolution of temperature at selected depth; *X*-axis refers to longitude, *Y*-axis to latitude; crosses indicate location of data used for interpolation (also shown in the corner right inset). (b) Evolution of conductivity (at 25 °C) as a function of depth; same symbolism as for Fig. 9a.

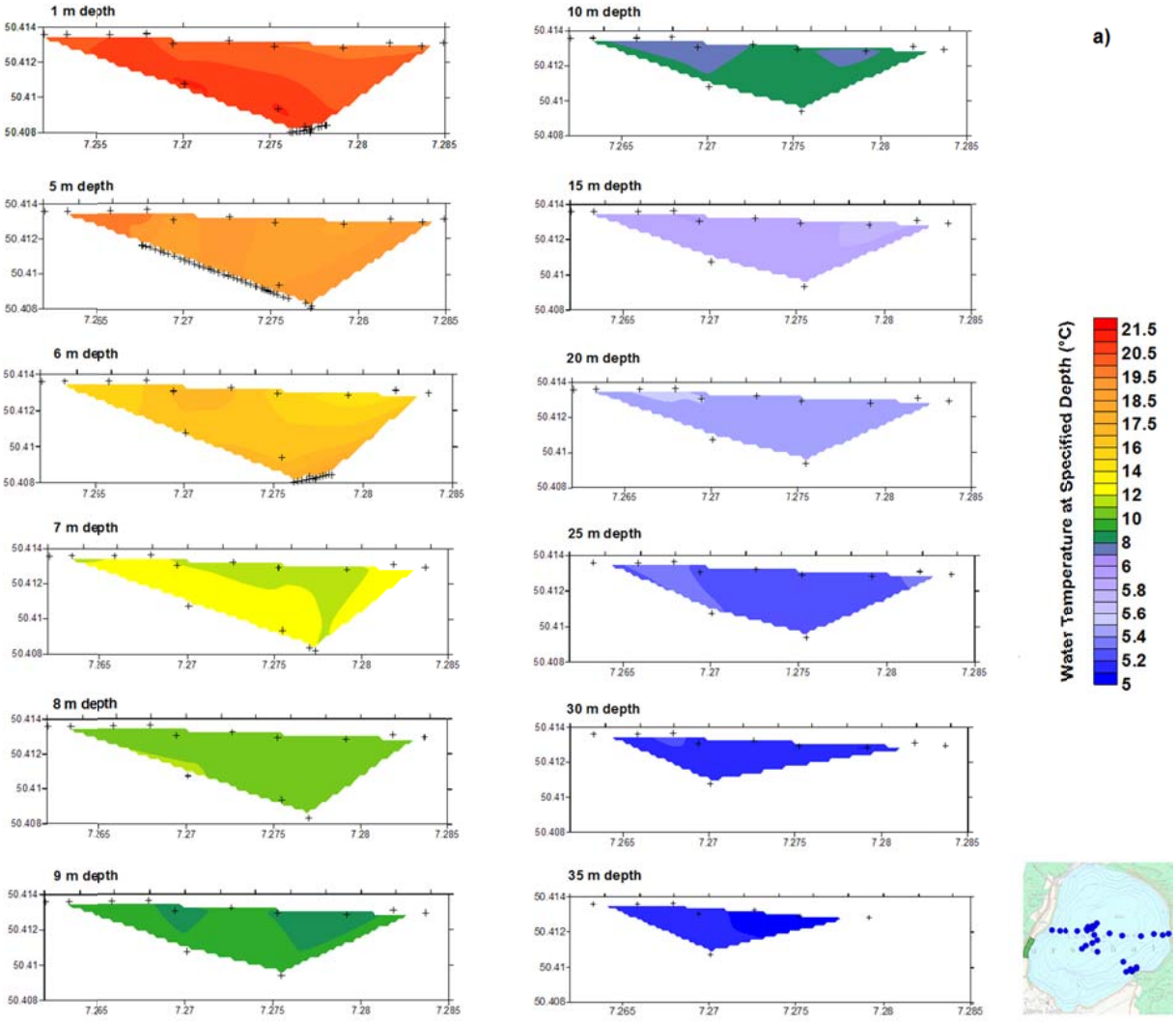
a)
1 m depth
5 m depth
6 m depth
7 m depth
8 m depth
9 m depth
10 m depth
15 m depth
20 m depth
25 m depth
30 m depth
35 m depth
50.414
50.412
50.41
50.408
7.265
7.27
7.275
7.28
7.285
Water Temperature at Specified Depth (°C)
21.5
20.5
19.5
18.5
17.5
16
14
12
10
8
6
5.8
5.6
5.4
5.2
5

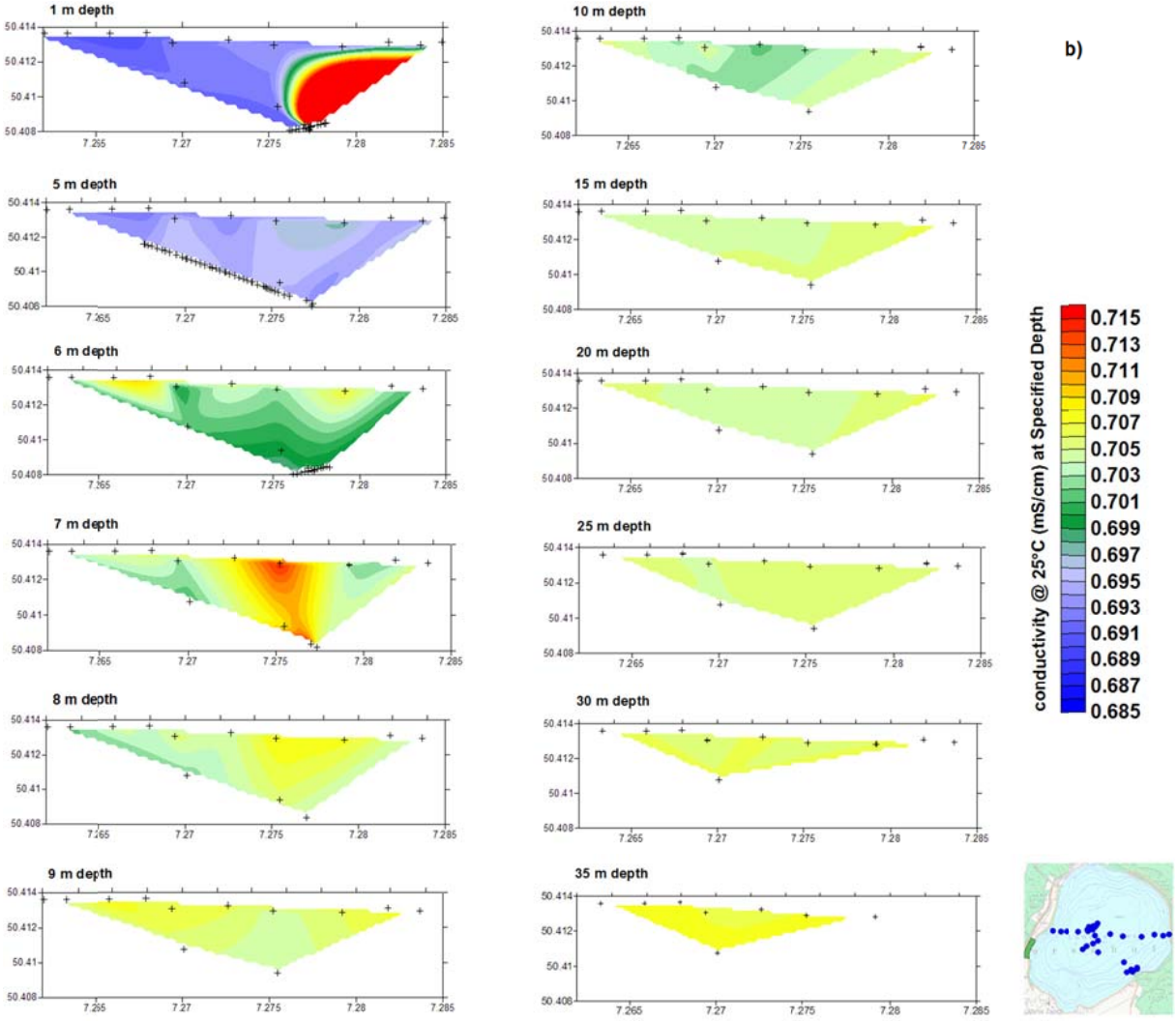

Conductivity changes with depth (Figures 8 and 9b) were scarce as they ranged between 690 and 715 µS/cm (at 25°C). In the firsts 5 m, the lower conductivities were recorded probably resulting from efficient mixing (wind forcing) and relative dilution due to surface waters, especially rainfalls supply. One exception was the occurrence of 'high' conductivities near the eastern shore at one meter depth, in an area where gas bubbling occurs (Figure 1). Such an increase of the conductivity when CO_2 is present as a gas phase has already been stated when testing the probe in the Détente well (section 3.3; data not shown). Nevertheless this anomaly was only visible at 1 m depth and did not extend up to lake's bottom where the gas did escape.

Further depth, conductivity increase was associated with the temperature drop in the thermocline (Figure 8) with some lateral heterogeneity that may be linked to gas bubbles migration which is a spot process all over the lake (Figure 9b). Under 15 m in depth, the conductivity began to stabilise, as the temperature did. Penetration into sediments resulted in drastic increases of the conductivity.

pH values ranged from slightly basic ones (8.5) at surface to near neutral ones at depth (Figures 8 and 10). Most changes occurred in the thermocline and in the hypolimnion, the upper 5 m experiencing only slight decrease of the pH value. Scarce influence of CO_2 degassing could be highlighted at 3 – 4 m depth near the Eastern shore where decreases of 0.2 to 0.5 pH units occurred between restricted water levels. Within the thermocline pH evolution was correlated with that of dissolved oxygen (Figure 8). This evolution should be linked to photosynthetic processes that are frequent in stratified lakes (Assayag *et al.*, 2008). Two significant rises of the pH were noted between 6 – 8 m depth (+ 0.1 pH unit) and 9 – 11 m depth (+ 0.6 to 0.7 pH units), corresponding to increases of respectively 150-200 and ~10% of the dissolved oxygen content. The thermocline is indeed characterised by a low transport by turbulent dispersion. The resulting confined zone it represents allows the accumulation of oxygen, effect of photosynthetic activity being greater. Below the thermocline, pH values again decreased, lower part of the lake showing homogeneous water body. Even if measurements were performed during long sunshine duration days, light penetration at great depth is not sufficient to allow strong photosynthetic activity. As a consequence, respiration processes – organic matter oxidation – become dominant and contribute to lower both pH and dissolved oxygen values. Nevertheless some lateral variations did exist on pH between 15 and 35 m depth. These lateral variations suggest a slight acidification of the external parts of the lake while horizons overlying the deepest part of the maar appear to be more basic (Figure 10a). Such lateral variations can be partly explained by divers' observations reported by Aeschbach-Hertig *et al.* (1996) who evidenced fast dissolution of bubbles coming from lake's bottom near 25 m depth in. As this 15 – 35 m depth sequence is very important towards carbon species, those variations can impact the depth were the waters become undersaturated versus dolomite (pH < 7.86), aragonite (pH <7.67) and calcite (pH < 7.51). Below 35 m depth, lake water was always undersaturated towards these species.

Figures 10a, b, c, d

Figure 10a: interpolation map: evolution of pH as a function of depth; same graphical chart as in Figure 9a.

Figure 10b: evolution of dissolved oxygen as a function of depth; same graphical chart as in Figure 9a.

Figure 10c: evolution of redox potential as a function of depth; same graphical chart as in Figure 9a.

Figure 10d: evolution of dissolved CO_2 (expressed as an electrical potential value – warning: the absolute value is taken) as a function of depth; same graphical chart as in Figure 9a.

Figure 11: schematic representation of the CO_2-rich areas around or in the Laacher See; labels 19, 27 and 29 refer to bibliographic references.

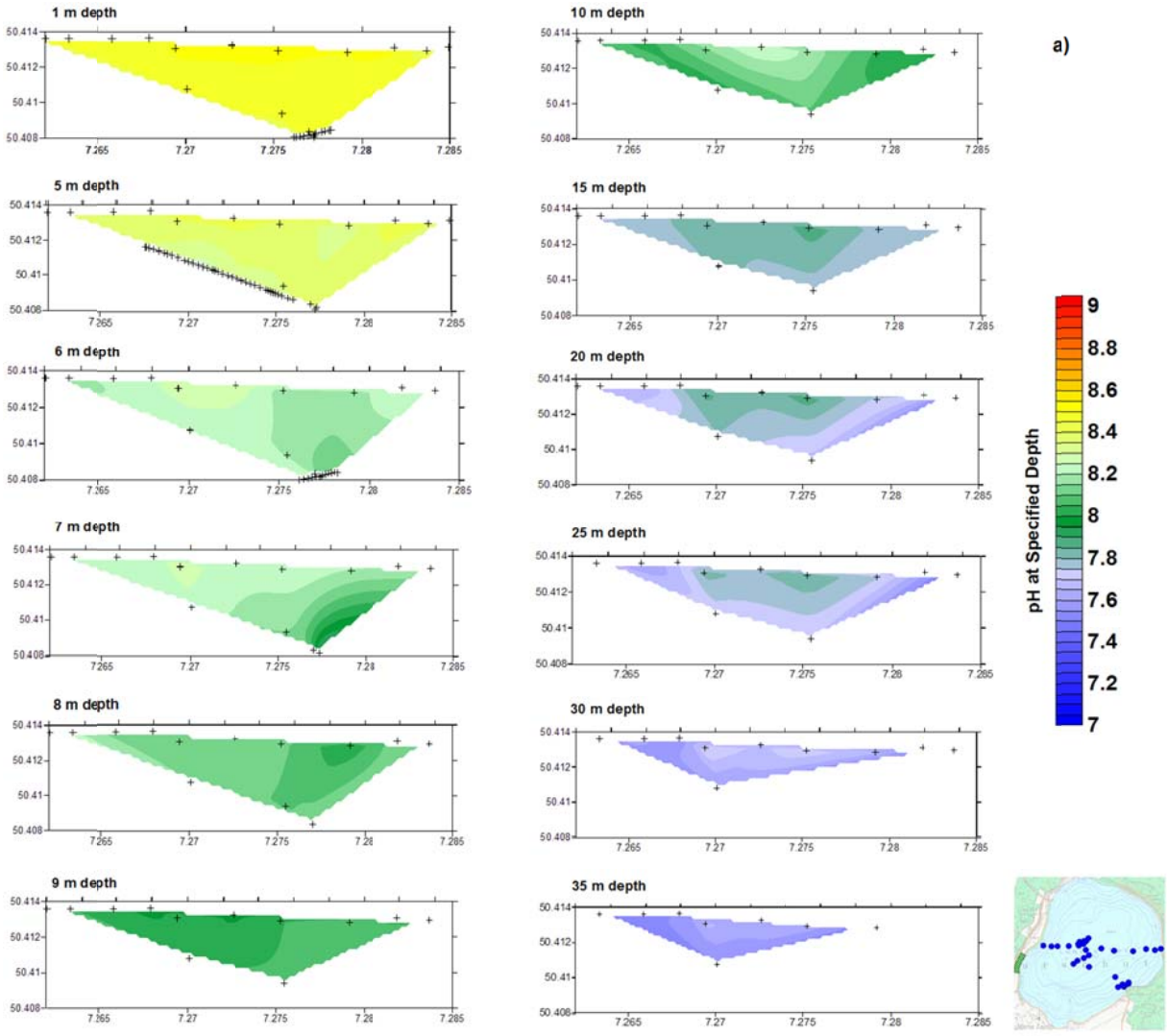

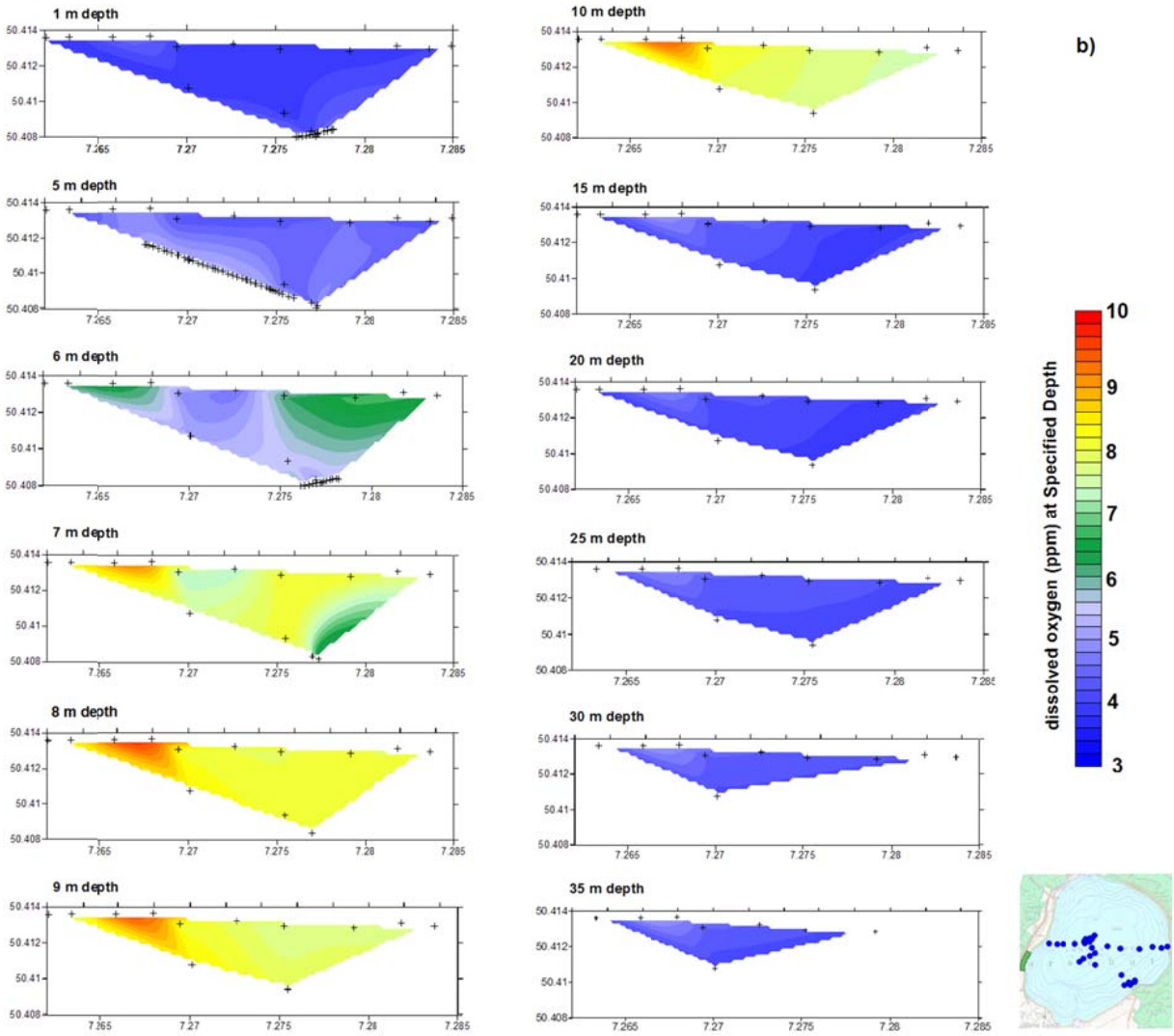
b)
1 m depth
5 m depth
6 m depth
7 m depth
8 m depth
9 m depth
10 m depth
15 m depth
20 m depth
25 m depth
30 m depth
35 m depth
50.414
50.412
50.41
50.408
7.265
7.27
7.275
7.28
7.285
dissolved oxygen (ppm) at Specified Depth
10
9
8
7
6
5
4
3

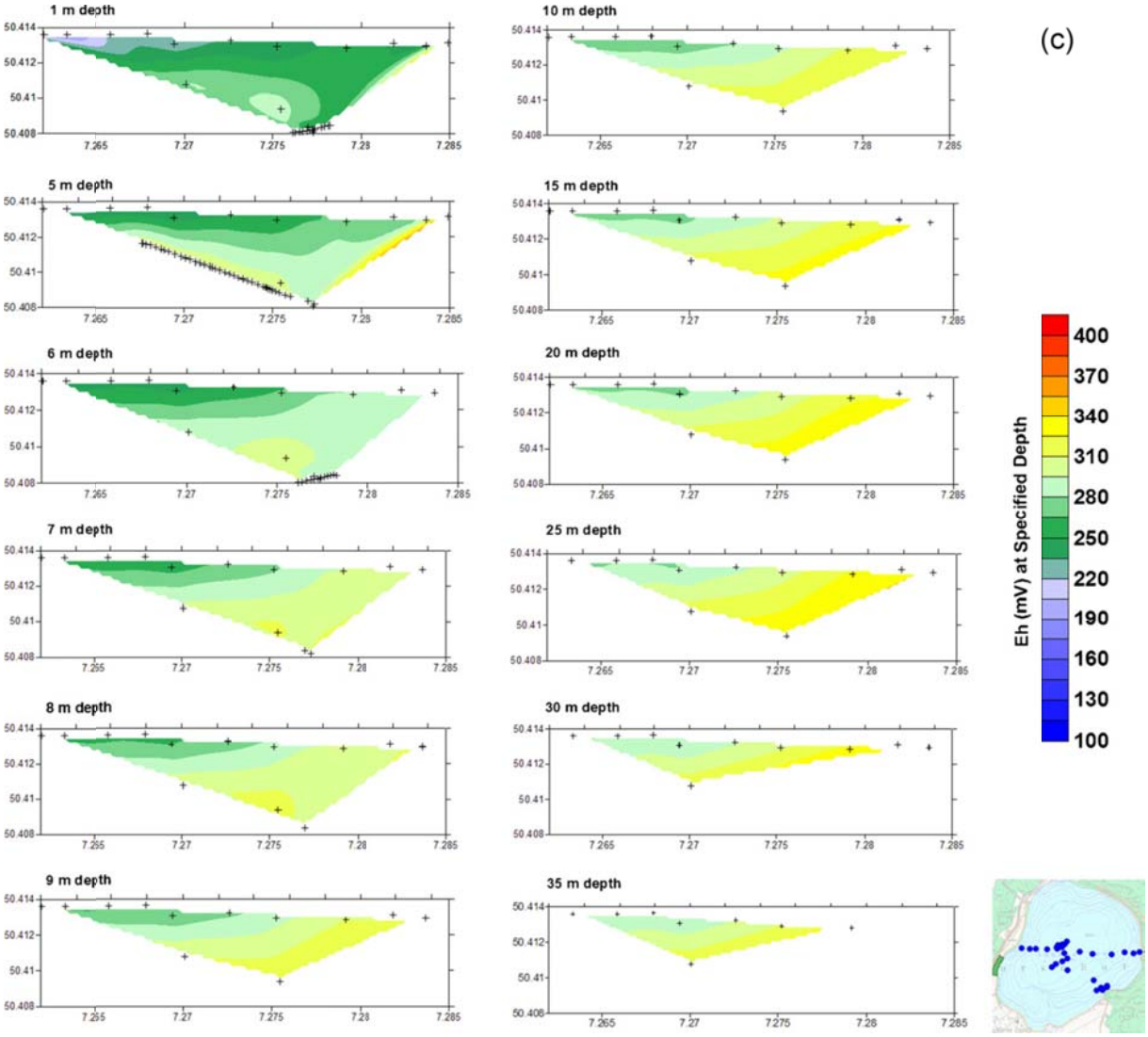
(c)
1 m depth
5 m depth
6 m depth
7 m depth
8 m depth
9 m depth
10 m depth
15 m depth
20 m depth
25 m depth
30 m depth
35 m depth
50.414
50.412
50.41
50.408
7.265
7.27
7.275
7.28
7.285
Eh (mV) at Specified Depth
400
370
340
310
280
250
220
190
160
130
100

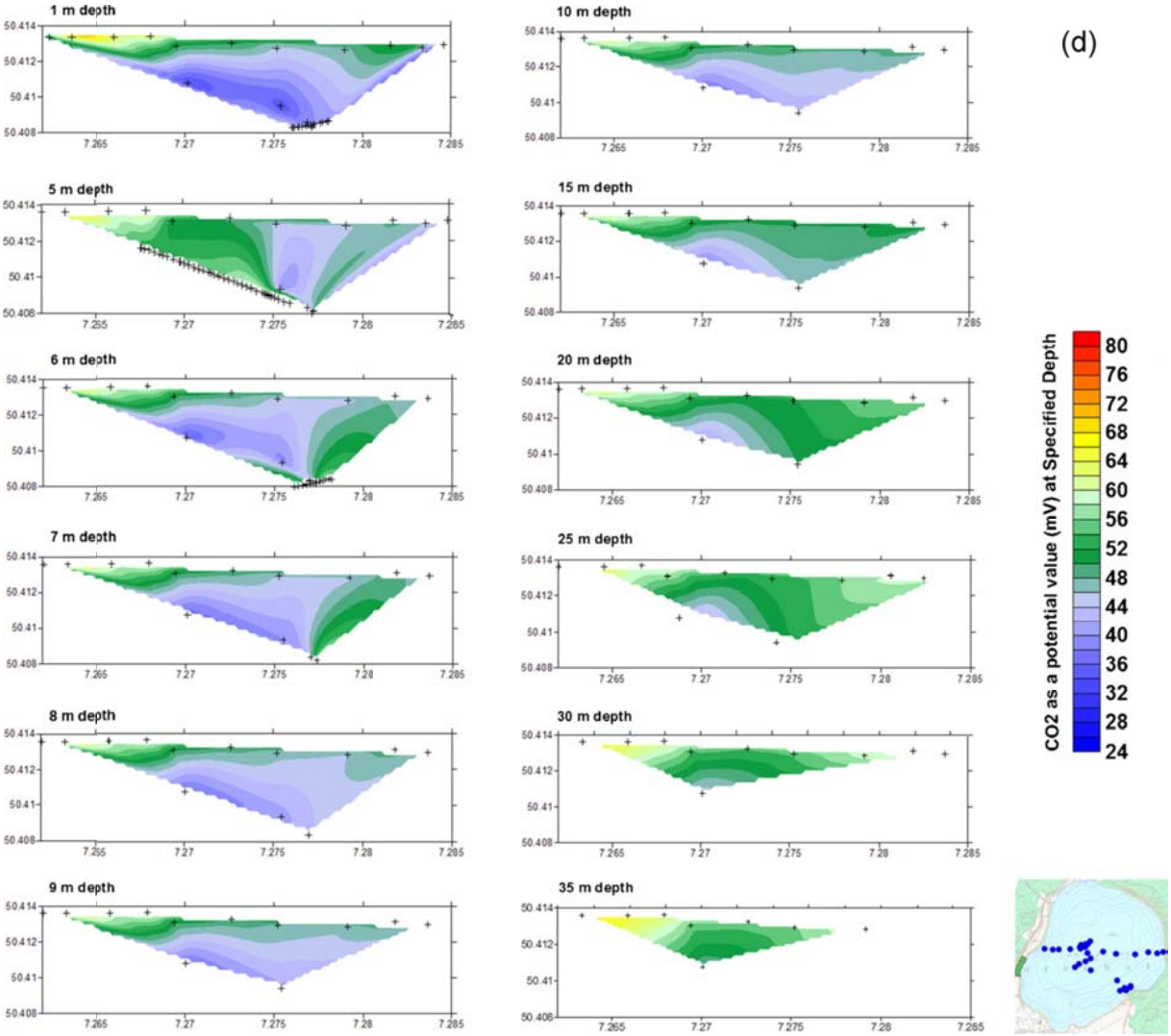

Redox potential showed gradual increase along the water column (Figures 8 and 10c) without relation to the different lake's compartments (epilimnion, thermocline, hypolimnion), rather showing a rapid increase of the potential from 0 to 10 m depth (+ 60 mV) and a gentle raise under 10 m depth (+ 20 mV down to bottom). A sudden decrease was stated when penetrating into unconsolidated sediments when the medium became reducing. At greater scale, logs performed along the Eastern shoreline suggested the presence of more oxidant waters than those encountered in the centre or near the Western shoreline especially in near surface horizons. Those parts of the lake being subject of CO_2 degassing, this was quite unexpected as the presence of a gaseous phase should strengthen oxygen stripping and consequently lower redox values.

As a consequence the entire water column was dominated by oxidant conditions but showed significant changes with depth (Figures 8 and 10b). Dissolved oxygen greatly evolved within the

thermocline, surface waters being less rich than thermocline waters and having same contents than deeper horizons. The 6 – 10 m depth interval was characterised by oxygen rich waters, especially on the Western part of the lake. This sudden dissolved oxygen change is not only related to the large temperature drop (a fall of 13 to 14°C) in the thermocline, which would favour gas dissolution, as the water below 15 m depth had a lower temperature and also a lower dissolved oxygen content. It should also be a consequence of the strong photosynthetic activity within this low turbulent dispersion zone (Jézéquel *et al.*, 2009). In areas where CO_2 escapes as a gas phase, a lesser oxygen content was from place to place measured, maybe related to stripping processes, but this statement contradicts the one made using redox data. Nevertheless dissolved oxygen contents were comparable to those found on collected water samples (Table 5). They also exhibited a downward evolution mimicking the one reported by Rheinland-Pflaz water authorities (data not shown – database from 2005 to 2007 made available courtesy of I. Möller, Bundesanstalt für Geowissenschaften und Rohstoffe, BGR, Hannover), the levels around 10 m depth in having dissolved oxygen contents reaching 1.5 to 3 times the concentrations existing at the surface or at 20 m depth (depending on the season). Such stratification is also stated in Lake Pavin where thermocline waters are enriched in dissolved oxygen (Assayag *et al.*, 2008).

Table 5

Dissolved gas contents (mol/l) measured on water samples taken from 10 to 46 m depth in the water column. LSX refer to samples location as indicated in Fig. 1; depth is indicated after hyphen; l.d.: limit of detection; l.q.: limit of quantification; n.d.: non-detected.

	CO_2	Ar	O_2	N_2	CH_4
LS4-10m	1,40E-04	6,30E-05	2,10E-03	9,90E-03	9,80E-08
LS4-20m	2,40E-04	2,30E-05	6,60E-05	9,10E-04	1,80E-08
LS3-30m	5,80E-04	1,40E-04	3,30E-03	1,20E-02	6,50E-08
LS4-30m	2,60E-04	2,10E-05	1,20E-04	8,60E-04	n.d.
LS4-40m	5,10E-04	2,20E-05	6,80E-05	1,20E-03	n.d.
LS2-45m	1,20E-03	6,20E-05	9,70E-04	5,40E-03	2,10E-08
LS4-46m	1,20E-03	2,40E-05	3,00E-05	1,20E-03	n.d.
l.d.	*3,50E-08*	*1,20E-08*	*1,10E-08*	*1,10E-08*	*2,20E-09*
l.q.	*5,30E-07*	*1,70E-07*	*1,70E-07*	*1,60E-07*	*3,30E-08*

Qualitative evolution of dissolved CO_2 contents (Figures 8 and 10d) suggested the presence of CO_2-rich waters on the Western part of the lake, and less enriched waters in the Eastern part, except some higher values between 5 to 7 m depth. This statement contradicts information inferred from chemical

analyses (table 4), in-situ sampling (table 5) and man eye observations. It's also in conflict with photosynthetic/respiration processes evolution along the water column, as the diminution of these processes should lead to CO_2 consumption and O_2 production rather than to CO_2 enrichment. No such O_2 enrichment is stated (Figure 10b). Moreover, the sensor did not react when immersed in lake compartments where bubbling occurs. The unique tendency that could partly reflect real processes is best highlighted by Figure 8, where CO_2 contents appeared to be greater at depth that in upper levels but far from concentrations really measured on samples (Table 4). For some of the profiles (labelled 5, 6 and 7), the minimum potential was recorded at depths where dissolved oxygen contents reached their maximum, which was a coherent behaviour. Last, there was another slight tendency exhibited by the sensor, consistent with a better CO_2 dissolution at depth where temperatures are colder than near the surface (Diamond and Akinfiev, 2003). As a consequence, and despite the information gathered during preliminary testing (eq. 1), data provided by this pCO_2 sensor are not enough reliable and too much dependent from depth and logging duration (*e.g.* for log 5 – 49 m depth, Pearson's coefficients are 0.970 for CO_2-depth and 0.956 for CO_2-time). Therefore, evolution of the water CO_2 content within the lake must be based on sampling and subsequent gas analyses.

The carbonate system in the Laacher See should be principally dependent from the pH value (Stumm and Morgan, 1981), as waters evolve from relatively alkaline type at surface to nearly neutral one at depth. This progressive decrease of the pH values is mainly related to the growing content of H_2CO_3, as the CO_3 content becomes smaller with depth and the alkalinity (expressed as the HCO_3 content) remains stable (Table 4). Hence, there is a progressive increase of the partial CO_2 pressure along with depth, and some local enrichments in the dissolved CO_2 are encountered in areas where bubbling occurs (sample LS5 bubbles in Table 4). Even in near surface waters (1.7 m depth), there is a slight CO_2 enrichment towards the atmospheric equilibrium concentration, but the increasing gradient down to bottom is far from the one observed in Lake Pavin by Aeschbach-Hertig *et al.* (1999). The absence of lake water stratification, especially the absence of a monimolimnion, only allows the CO_2 equilibrium partial pressure to reach 0.023 atm at lake's bottom. Depending on dissolved species, this pressure is still higher than the one calculated for Lake Pavin at similar depth (again 3 times enrichment) but does not favour at all degassing of the water. CO_2 remains far from saturation in the deepest parts of the lake (saturation concentration c.a. 94 mmol/l; Diamond and Akinfiev, 2003). There is no evidence of

degassing from the water body itself, all the bubbling coming from demixtion processes occurring deeper in the earth crust.

As often stated (Bakalowicz, 1994), CO_2 concentrations measured on samples (Table 5) are smaller than the ones coming from calculations (taken as the H_2CO_3 total content, i.e. the sum of $CO_{2(aq.)}$ and H_2CO_3), but the highest discrepancy is lesser than a 2 times underestimation, and sometimes higher CO_2 contents are determined by the sampling method. As a consequence, we would no reject these analyses, as made by Aeschbach-Hertig *et al.* (1999) using data from Camus *et al.* (1993) concerning Lake Pavin. Moreover the total H_2CO_3 content takes into account both the $CO_{2(aq.)}$ and H_2CO_3 contributions and can therefore explain, at least partially, the gap between the two dissolved CO_2 evaluations. Around 45 m depth, there is a good agreement between the two methods, calculations leading to a 0.975 – 1.485 mmol/l content, whereas two direct measurements give the same content (1.2 mmol/l), which is identical to the mean value arising from equilibrium considerations. Taking into account huge errors affecting these considerations (± 20 %; Aeschbach-Hertig *et al.*, 1999), such an agreement should indicate that the sampling procedure and subsequent gas analyses fairly reflect the real dissolved gas contents.

Other detected gases were atmospheric ones (O_2, Ar, N_2) and punctually CH_4 (Table 5). Sample LS3-30m has been affected by sampling bias during sample recovery, its O_2 and N_2 contents reaching or exceeding gas saturation at specified temperature (saturation concentrations under atmospheric equilibrium: 3.5E-03 and 2.2E-03 mol/l respectively; Weiss, 1970). In lesser extent, same statement can be done for the 10 m depth sample, where N_2 was close to saturation. Secondary O_2 enrichment was stated near 30 m depth, accordingly with shapes illustrated by Figure 8. Remaining samples are far from saturation concentrations and showed a rather constant evolution along with depth except some higher values near the lake's bottom (45 m) that were not confirmed 1 meter deeper (46 m). Very low amounts of CH_4 were measured from time to time with no consistent evolution with depth. The presence of CH_4 can be linked to the biological state of the lake (mesotrophic to eutrophic).

As a consequence, the dissolved gas measurements all suggest a strong influence of the atmospheric compartment, probably linked to seasonal overturn(s) experienced by the whole water body. Underwater seepages were not clearly highlighted at the centre of the lake and the ones occurring on the Eastern shore did not have noticeable influence several hundreds of meters further to the West (Figure 11). Especially, the CO_2 gas vents emplaced along the Western shore do not have noticeable

effects on the water chemistry, whereas the CO_2 present along the Eastern shore imprints both the water chemistry and the soil gas contents. Nevertheless, the influence of this degassing appears to be restricted to surface water horizons (0 – 10 m depth), which are more sensitive to small chemical changes.

Figure 11

Schematic representation of the CO_2-rich areas around or in the Laacher see references ([Jones et al., 2009] and [Langer, 1988]).

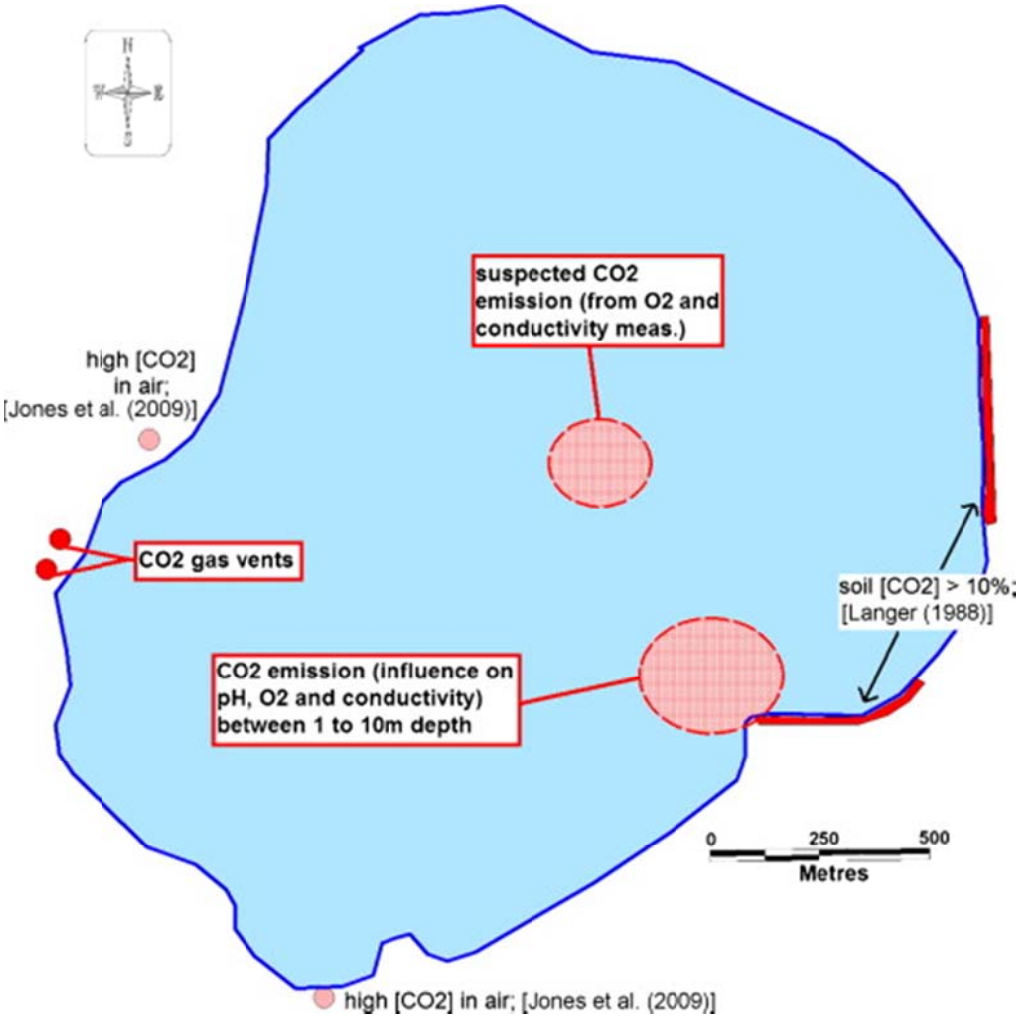

6. Conclusion: what can be learned from CO_2 escapes in the Laacher See region?

This study of the Laacher See water body and its surroundings has dealt with two sets of monitoring approaches, based on terrestrial and offshore monitoring methods.

Terrestrial applications highlight the occurrence of several gaseous releases, with dominant CO_2 content (Figure 11). Some of them are clearly distinguishable within the environment (absence of grassland or presence of different grass species) whereas others can only be detected using in-situ gas analyses. Most of the known degassing structures around the lake are oriented along an N-S axis, which is consistent with the known geological structuration of the hercynian basement. Radon and helium were systematically co-eluted with this CO_2 phase. Radon transportation depends on the CO_2 flux but also on the soil mineral composition. In the areas with prominent CO_2 gas phase originated from depth, the relationship between CO_2 (vector phase) and the radon is less satisfactory than in areas with lesser CO_2 amounts. Whatever the radon production rate is, the existence of anomalies at 1 m depth in soils greatly depends on the velocity of the CO_2. In areas where the uprising flux is high, radon activities can be lowered as radon production is not high enough to supply amounts proportional to those of the CO_2. Moving away from mofettes centres, the CO_2 flux diminishes, but the radon exhalation should remain nearly the same in a few meters interval. The relationship between the two gases will then be different from the one stated in the centre of the gas vent. As a result, matrix calculations performed on the entire dataset, suggest a relatively poor relationship between CO_2 and radon, at least poorer than relationships that can be drawn for areas where deep gas influx are not known (Gal *et al.*, 2010). Same statement can be made using helium, even if this gas phase also comes from depth. A dilution effect should lower the helium concentrations at the apex of the gas vent, and have a lesser influence when moving outwards.

Offshore applications consisted in lake water monitoring and have revealed a homogeneous thermal stratification from the western to the eastern shorelines, with a rather constant electrical conductivity in the water column. This conductivity is quite high for lake waters emplaced in such geological environments and may be partly related to lake feeding by mineral water leaks, as is postulated for lake Pavin (Jézéquel *et al.*, 2009). Nevertheless, such seepages had neither been highlighted during the cruises made using Idronaut probe nor were able to explain the significant chlorine enrichment found in the samplings. Substantial bicarbonate content was found all along the water column, reaching levels rather characteristic of monimolimnion environments (e.g. lake Pavin) than purely freshwater feeding in non-sedimentary areas. Chemical equilibrium relationships for the carbonate system, as well as in-situ gas and water sampling, also suggested a gradual and progressive increase of the dissolved CO_2 content with depth. This may be linked to dissolution of CO_2 gas coming from

non-thermally disturbing underwater releases but these releases – which did exist as they are visible at the lake's surface (Figure 11) – had low to very low impact on water electrical conductivity. From place to place pH parameter may be more impacted by the CO_2 but there may be an overlap with photosynthetic processes – and with O_2 production/consumption processes – which were not accounted for during this study. As no strong degassing areas were highlighted in the centre of the lake, nor potential underwater seepage, it was not possible to locate preferential leaking pathways beneath the lake bottom in its deeper parts.

In view of characterising, monitoring and subsequently insuring of the safety of CO_2 underground geological storages, above described results lead to the following comments:

- As structural control of potential leaks is one of the major issues to be addressed, one may be sufficiently confident to the ability of geochemical surveying methods to detect any variability of the fluid composition that may be related to processes other than naturally occurring ones. In the present case, a distinction has to be made between the lake itself and its surroundings. As in other locations, onshore monitoring methods allow to highlight areas with gas releases greater than the environmental background and to define the migration pathways in terms of intensity of gas feeding, using several species (*e.g.* CO_2, He, ^{222}Rn) of different behaviours.
- Assessing the behaviour of gas releases in water bodies is much more complicated. Here we have used logging probes and sampling to the characterisation of the Laacher See which is an open water body that is easier to survey that groundwaters and deep aquifers. Even in such preferential conditions, it is highly difficult to clearly advocate of the location of deep gas and/or other fluid feedings. Indeed the surveying of open waters adds many contingencies that do not exist at deeper horizons, such as photosynthetic processes in the present case, but interrogations may exist regarding the capacity to highlight small variations in deeper aquifers and link them to CO_2 storage operations.
- Especially, as long-term monitoring is highly desirable, there is a complementary requirement that may not be totally addressed until now concerning the technological gap that exists for some monitoring parameters, such as months-long pH, dissolved oxygen or redox potential measurements. Long-term gas monitoring in the unsaturated zone or at the soil/atmosphere

interface is presently better technically constrained as sensor drifting may be overcame or biofouling effects may have lesser impacts on measurements.

As a consequence, geochemical monitoring techniques that are to be used for CO_2 storage characterisation and surveying must focus on several aspects rather than simply relying to a unique set of methods (i.e. focus on gas or water surveying). Gas monitoring with surface techniques would only be relevant if there are some geological structures that may allow gas migration. At the opposite, gas and water monitoring at depth, through dedicated monitoring boreholes, may allow to monitor gas migration *e.g.* via regular water logging, but suffers from a major drawback as boreholes only represent punctual structures compared to storage size. Despite this disadvantage, geochemical monitoring must be envisaged in such CO_2 storages, as it is the only method that is able to evaluate chemical changes resulting from CO_2 injection, as geophysical methods are best suited for monitoring plume migration along time.

Acknowledgments

Financial support was get from the European Commission under the Contract SES6-CT-2004-502816, "Network of Excellence on CO_2 geological storage - CO_2GeoNet April 2004 - March 2009". Additional funding was get from authors' institution under BRGM/METRENV project. The authors would also highlight fruitful cooperative work with people from other institutions (BGR, BGS) during field surveys. F. May and I. Möller (BGR) are gratefully acknowledged for their availability and help during the two campaigns. Analyses were performed at BRGM by C. Flehoc (carbon isotopes), B. Henry (gas chromatography), A. Gautier and S. Touzelet (cations/anions analyses).

References

Aeschbach-Hertig W., Kipfer R., Hofer M., Imboden D.M., Wieler R., Signer P. (1996) Quantification of gas fluxes from the subcontinental mantle: The example of Laacher See, a maar lake in Germany, Geochimica et Cosmochimica Acta, Vol. 60, No. I, 31-41.

Aeschbach-Hertig W., Hofer M., Kipfer R., Imboden D.M., Wieler R. (1999) Accumulation of mantle gases in a permanently stratified volcanic lake (Lac Pavin, France, Geochimica et Cosmochimica Acta, Vol. 63, No. 19/20, 3357-3372.

Aiuppa A., Baker D.R., Webster J.D. (2009) Halogens in volcanic systems, Chem. Geol. 263, 1-18

Assayag N., Jézéquel D., Ader M., Viollier E., Michard G., Prévot F., Agrinier P. (2008) Hydrological budget, carbon sources and biogeochemical processes in Lac Pavin (France): Constraints from $\delta^{18}O$ of water and $\delta^{13}C$ of dissolved inorganic carbon, Applied Geochemistry, 23, 2800–2816.

Bahrig B. (1985) Sedimentation und Diagenese im Laacher Seebecken (Osteifel). – Bochumer Geol. u. Geotechn. Arb. 19. 231 pp.

Bakalowicz M. (1994) Water geochemistry: water quality and dynamics, In Groundwater Ecology, Academic Press Eds., 97-127

Battani A., Deville E., Faure J-L., Noirez S., Tocqué E., Jeandel E., Benoît Y., Schmitz J., Parlouar D., Gal F., Le Pierrès K., Brach M., Braibant G., Bény C., Pokryszka Z., Charmoille A., Bentivegna G., Pironon J., de Donato P., Garnier C., Cailteau C., Barrès O., Radilla G., Bauer A. (2010) Geochemical study of the natural CO_2 emissions in the French Massif Central : How to predict origin, processes and evolution of CO_2 leakage, Oil & Gas Science and Technology, Special issue on CO_2 Storage in the Struggle against Climate Change, 65, 4, 615-633.

Baubron J.C., Rigo A., Toutain J.P., 2002. Soil gas profiles as a tool to characterise active tectonic areas: the Jaut Pass example (Pyrenees, France). Earth and Planetary Science Letters 196, 69–81.

Beaubien S.E., Ciotoli G., Coombs P., Dictor M.C., Krüger M., Lombardi S., Pearce J.M., West J.M. (2008) The impact of a naturally occurring CO_2 gas vent on the shallow ecosystem and soil chemistry of a Mediterranean pasture (Latera, Italy). International Journal of Greenhouse Gas Control, 2, 373 – 387.

van den Bogaard P. (1995) $^{40}Ar/^{39}Ar$ ages of sanidine phenocrysts from Laacher See Tephra (12,900 yr BP): Chronostratigraphic and petrological significance, Earth and Planetary Science Letters, 133, 163-174

Camus G., Michard G., Olive P., Boivin P., Desgranges P., Jézéquel D., Meybeck M., Peyrus J.-C., Vinson J.-M., Viollier E., and Kornprobst J. (1993) Risques d'éruption gazeuse carbonique en Auvergne, Bull. Soc. Géol. France 164, 767–781, in French.

Ciotoli G., Etiope G., Guerra M., Lombardi S., 1999. The detection of concealed faults in the Ofanto Basin using the correlation between soil-gas fracture surveys. Tectonophysics 301, 321-332.

Czernichowski-Lauriol I., Arts R., Durand D., Durucan S., Johannessen P., May F., Olivier M.L., Persoglia S., Riley N., Sohrabi M., Stokka S., Vercelli S., Vizika-Kavvadias O. (2009) CO2GeoNet, the unique role of the European scientific body on CO2 geological storage, GHGT-9, Energy Procedia, 1, 2043–2050.

Diamond L.W. and Akinfiev N.N. (2003) Solubility of CO_2 in water from -1.5 to 100°C and from 0.1 to 100Mpa: evaluation of literature data and thermodynamic modelling, Fluid Phase Equilibria 208, 265-290

Etiope G., Martinelli G. (2002) Migration of carrier and trace gases in the geosphere: an overview, Physics of the Earth and Planetary Interiors, 129, 185–204.

Finkelstein M., Brenner S., Eppelbaum L., Ne'eman E. (1998) Identification of anomalous radon concentrations due to geodynamic processes by elimination of Rn variations caused by other factors, Geophys. J. Int., 133, 407-412

Gal F., Le Pierrès K., Brach M., Braibant G., Beny C., Battani A., Tocqué E., Benoît Y., Jeandel E., Pokryszka Z., Charmoille A., Bentivegna G., Pironon J., de Donato P., Garnier C., Cailteau C., Barrès O., Radilla G., Bauer A. (2010) Surface gas geochemistry above the natural CO_2 reservoir of Montmiral (Drôme-France), source tracking and gas exchange between soil, biosphere and atmosphere, Oil & Gas Science and Technology, Special issue on CO_2 Storage in the Struggle against Climate Change, 65, 4, 635-652.

Gale J. (2004) Geological storage of CO_2: what do we know, where are the gaps and what more needs to be done? Energy, 29, 9-10, 1329-1338.

Gapillou C., Thibeau S., Mouronval G., Lescanne M. (2009) Building a geocellular model of the sedimentary column at Rousse CO_2 geological storage site (Aquitaine, France) as a tool to evaluate a theorical maximum injection pressure, GHGT 9. Energy Procedia, 1, 2937–2944.

Giggenbach W.F. (1990) Water and gas chemistry of Lake Nyos and its bearing on the eruptive process, In: F. Le Guern and G.E. Sigvaldason (Editors), The Lake Nyos Event and Natural CO_2 Degassing, II, J. Volcanol. Geotherm. Res., 42, 337-362

Giggenbach W.E, Sano Y., Schmincke H.U. (1991) CO_2-rich gases from Lakes Nyos and Monoun, Cameroon; Laacher See, Germany; Dieng, Indonesia, and Mt. Gambier, Australia – variations on a common theme. J. Volcanol. Geotherm. Res., 45, 311-323.

Griesshaber E., O'Nions R.K., Oxburgh E.R. (1992) Helium and carbon isotope systematics in crustal fluids from the Eifel, the Rhine Graben and Black Forest, F.R.G. – Chem. Geol. 99, 213-235.

Heinicke J., Koch U., Martinelli G. (1993) Simultaneous measurements of radon and CO_2 in spring water for earthquake prediction research, Proceedings of the Scientific meeting on the seismic protection, Venice 12-13 July 1993, 152-155

Holloway S., Pearce J.M., Hards V.L., Ohsumi T., Gale J. (2007) Natural emissions of CO_2 from the geosphere and their bearing on the geological storage of carbon dioxide. Energy, 32, 1194–1201

Iundt F. and Robalo J. (1990) Evolution naturelle de l'eau du nouveau forage thermal – Optimisation de son exploitation, rapport BRGM R-30771-RHA-4S-90, 10p., 3 fig. + ann. , in French.

Jézéquel D., Albéric P., Binet S., Sarazin G., Prévot F., Viollier E., Groleau A., Jakubowski L., Boulanger E., Bergonzini L., Michard G. (2009) A contribution to the water budget of Lac Pavin, International Meeting Lake Pavin and Other Meromictic Lakes, May 14-15-16 2009, Besse et St Anastaise, France

Jones D.G., Barlow T., Beaubien S.E., Ciotoli G., Lister T.R., Lombardi S., May F., Möller I., Pearce J.M., Shaw R.A. (2009) New and established techniques for surface gas monitoring at onshore CO_2 storage sites GHGT-9, Energy Procedia 1, 2127-2134

Koehler G., Wassenaar L.I. (2010) The stable isotopic composition ($^{37}Cl/^{35}Cl$) of dissolved chloride in rainwater, Applied Geochemistry 25, 91-96

Krüger M., West J., Frerichs J., Oppermann B., Dictor M.C., Joulian C., Jones D., Coombs P., Green K., Pearce J., May F., Möller I. (2009) Ecosystem effects of elevated CO_2 concentrations on microbial populations at a terrestrial CO_2 vent at Laacher See, Germany, GHGT-9, Energy Procedia 1, 1933-1939

Kumar A., Singh S., Mahajan S., Singh Bajwa B., Kalia R., Dhar S. (2009) Earthquake precursory studies in Kangra valley of North West Himalayas, India, with special emphasis on radon emission, Applied Radiation and Isotopes, 67, 1904–1911

Langer M.A. (1988) CO2-Emissionen als Indikatoren tektonischer und vulkanotektonischer Störungen in der Osteifel. – Mitt. Pollichia 75: 127-142.

Pauwels H., Gaus I., Le Nindre Y.-M., Pearce J., Czernichowski-Lauriol I. (2007) Chemistry of fluids from a natural analogue for a geological CO_2 storage site (Montmiral, France): Lessons for CO_2–water–rock interaction assessment and monitoring, Appl.Geochem. 22, 2817-2833.

Renac C., Gal F., Ménot R.-P., Squarcioni P., Perrache Ch. (2009) Mean recharge times and chemical modelling transfers from shallow groundwater to mineralized thermal waters at Montrond-les-Bains, Eastern Massif Central, France, Journal of Hydrology, 376, 1–15

Riding J.B., Rochelle C.A. (2005) The IEA Weyburn CO_2 Monitoring and Storage Project, Final report of the European research team, British Geological Survey Research Report, RR/05/03, 54 p.

Severinghaus J.W. and Bradley A.F. (1958) Electrodes for blood P_{O2} and P_{CO2} determination, J. Appl. Physiol. 13, 515-520

Stumm W., Morgan J.J. (1981) Aquatic chemistry. An introduction emphasizing chemical equilibria in natural waters, 2nd Edition, 780 pp., J. Wiley & Sons, N.York.

Toutain J.-P., Baubron J.-C. (1999) Gas geochemistry and seismotectonics: a review, Tectonophysics, 304, 1–27.

Virk H.S., Walia V. (2001) Helium/radon precursory signals of Chamoli Earthquake, India, Radiation Measurements, 34, 379–384

Wattananikorn K., Kanaree M., Wiboolsake S. (1998) Soil gas radon as an earthquake precursor: some considerations on data improvement, Radiation Measurements, Vol. 29, No. 6, 593-598

Weiss R.F. (1970) The solubility of nitrogen, oxygen and argon in water and seawater, Deep-Sea Research, 17, 721-735.

Wildenborg T., Bentham M., Chadwick A., David P., Deflandre J.-P., Dillen M., Groenenberg H., Kirk K., Le Gallo Y. (2009) Large-scale CO_2 injection demos for the development of monitoring and verification technology and guidelines (CO2ReMoVe), GHGT 9. Energy Procedia, 1, 2367–2374.

Winthaegen P., Arts R., Schroot B. (2005) Monitoring Subsurface CO_2 Storage. Oil & Gas Science and Technology, 60, 3, 573-582.

Xue S., Dickson B., Wu J. (2008) Application of ^{222}Rn technique to locate subsurface coal heatings in Australian coal mines. International Journal of Coal Geology 74, 139-144.

Figure captions

Figure 1: site location: green dashed area: soil gas survey done in 2007; labelled yellow points: emplacement of CTD probe logging; labelled blue squares: in-situ water sampling location

Figure 2: a) evolution of the electrical response of the CO_2 sensor with time when exposed to progressive CO_2 enrichment (gas phase); b) and c): evaluation of the sensor's equilibration time: b) when exposed to tap water (low CO_2 content) at time 0 after equilibrating in CO_2-rich water; c) when exposed to injection of 10 % vol. of CO_2 gas in water (starting at time 0).

Figure 3: water logging of Détente well: plot vs. depth of water temperature, pH and CO_2 (as mV value); dashes along the depth axis figure the depths where stops were made during logging. Lower right graphs represent the variation of the CO_2 value as a function of water temperature and logging duration.

Figure 4: meteorological parameters (air temperature, rainfall amount, barometric pressure, sunshine duration and relative humidity) before and during the survey; data from Koblenz-Bendorf weather station, http://www.weatheronline.co.uk/.

Figure 5: plot of soil gas measurements vs. time of sampling.

Figure 6: soil gas species along the western shore of lake Laacher See. Interpolation is done using natural neighbour computation, and is only valid near the set of 86 measurements (location represented by dots on central inset). Location of the western shoreline of the lake is indicated. Grid scaling: 20 m interval.

Figure 7: Schöeller-Berkaloff diagram showing major ion contents of Erlenbrunnen mineral spring and Laacher See (LS) lake from near surface (-1.7 m) to bottom (-46 m); surface and bottom characteristics of Lake Pavin water (French Massif Central) are also indicated for comparison (BRGM, 2009, unpublished data).

Figure 8: synthetic view of deepest logs acquired in the Laacher See. Labels in captions refer to Figure 1. Data from May and September months are from Aeschbach-Hertig *et al.* [25]. The inset in O_2 vs. depth diagram shows the relationship between O_2 and pH.

Figure 9a: interpolation map drawn using the natural neighbour algorithm: evolution of temperature at selected depth; X-axis refers to longitude, Y-axis to latitude; crosses indicate location of data used for interpolation (also shown in the corner right inset).

Figure 9b: evolution of conductivity (at 25°C) as a function of depth; same symbolism as for Figure 9a.

Figure 10a: interpolation map: evolution of pH as a function of depth; same graphical chart as in Figure 9a.

Figure 10b: evolution of dissolved oxygen as a function of depth; same graphical chart as in Figure 9a.

Figure 10c: evolution of redox potential as a function of depth; same graphical chart as in Figure 9a.

Figure 10d: evolution of dissolved CO_2 (expressed as an electrical potential value – warning: the absolute value is taken) as a function of depth; same graphical chart as in Figure 9a.

Figure 11: schematic representation of the CO_2-rich areas around or in the Laacher See; labels 19, 27 and 29 refer to bibliographic references.

Tables

Table 1: Soil gas measurements statistics: a) Laacher See site; b) Obermendig site.

Table 2: Correlation matrix – all data (Pearson coefficient).

Table 3: gas chromatography results; samples location is indicated in Figure 3; d.l.: detection limit; precision of isotope ratio measurements is ± 0.1‰ VPDB.

Table 4: chemical analyses of Laacher See water and Erlenbrunnen mineral spring; chemical balances are in the range -2 to +4%. For samples LSX refer to Figure 1 for location; sampling depth is indicated after the hyphen. Saturation index (SI) and mmol/l concentrations of carbonated species (TDIC = Total Dissolved Inorganic Carbon = H_2CO_3 + HCO_3 + CO_3) are computed using Diagramme software (http://www.lha.univ-avignon.fr/LHA-Logiciels).

Table 5: dissolved gas contents (mol/l) measured on water samples taken from 10 to 46 m depth in the water column. LSX refer to samples location as indicated in Figure 1; depth is indicated after hyphen; l.d.: limit of detection; l.q.: limit of quantification; n.d.: non detected.